AUS DER ABTEILUNG
FÜR PLASTISCHE, HAND- UND WIEDERHERSTELLUNGSCHIRURGIE
PROF. DR. UNIV. DR. LUKAS PRANTL
DER FAKULTÄT FÜR MEDIZIN
DER UNIVERSITÄT REGENSBURG

APPLICATION OF ADIPOSE TISSUE-DERIVED STEM CELLS FOR RESTORATION OF ACHILLES TENDON ELASTICITY AFTER INJURY

DISSERTATION

zur Erlangung des Doktorgrades
der Medizin
(doctor medicinae)

der
Fakultät für Medizin
der Universität Regensburg

vorgelegt von
Tobias Kügler
geboren in Gräfeling
2017

GEWIDMET MEINEN ELTERN
UND MEINEM BRUDER NIKOLAI

Dekan: Prof. Dr. Dr. Torsten E. Reichert
1. Berichterstatter: Prof. Dr. univ. Dr. Lukas Prantl
2. Berichterstatter: Prof. Dr. Dr. Torsten E. Reichert
Tag der mündlichen Prüfung: 29.11.2017

Teile dieser Arbeit wurden publiziert:

Sebastian Gehmert, Ernst-Michael Jung, Tobias Kügler, Silvan Klein, Sanga Gehmert, Katharina Zeitler, Markus Loibl, Lukas Prantl: Sonoelastography can be used to monitor the restoration of Achilles tendon elasticity after injury Ultraschall Med. 2012 Dec; 33(6): 581-6

Außerdem wurden die Ergebnisse beim 42. Jahreskongress der Deutschen Gesellschaft der Plastischen, Rekonstruktiven und Ästhetischen Chirurgen in Innsbruck, Österreich 2011 in einer Präsentation vorgestellt:

Sebastian Gehmert, Tobias Kügler, Silvan Klein, Eckhard Alt, Michael Jung, Lukas Prantl. Autologe Stammzellapplikation unterstützt die Regeneration der Elastizität von Sehnengewebe.

Dokumentationsblatt

Bibliografische Beschreibung

Kügler, Tobias
Application of adipose tissue-derived stem cells for restoration of achilles tendon elasticity after injury
-2016.- 72 Bl., 16 Abb., 18 Tab.

Medizinische Fakultät der Universität Regensburg
Zentrum für Plastische, Hand- und Wiederherstellungschirurgie
(Direktor: Prof. Dr. univ. Dr. Lukas Prantl)

Kurzreferat:
Aktuelle Studien lassen darauf schließen, dass Stammzellen, isoliert aus dem Fettgewebe (adipose tissue-derived stem cells – ASCs), zur Behandlung von Sehnenrupturen verwendet werden können. Bisherige Ergebnisse belegen dies aufgrund von histologischen, immunhistologischen und verschiedensten biomechanischen Untersuchungen. Das Ziel dieser Arbeit war es zu untersuchen, ob die Behandlung von Achillessehnen mit ASCs zu einer Verbesserung der Elastizität führt und ob man diesen Effekt objektiv mit Hilfe der Sonoelastographie demonstrieren kann.
Es konnte gezeigt werden, dass Achillessehnen bei Behandlung mit ASCs auf einer Kollagenmatrix im Vergleich zu der Gruppe, behandelt nur mit Kollagenmatrix, einen signifikant niedrigeren Elastizitätsindex aufweisen konnten. Der Index-Wert entsprach dabei dem Niveau einer unverletzten Sehne. Weiterhin konnte dargestellt werden, dass die Sonoelastographie den Elastizitätsindex objektiv und valide abbilden kann.

Schlüsselwörter: **[Achillessehne], [adipose tissue-derived stem cells], [Elastizitaetsindex], [Sonoelastographie]**

Table of Contents

1. Zusammenfassung

Ziel: Die Sonoelastographie kann mechanische Eigenschaften von Gewebe darstellen und ist daher geeignet Defekt- und Narbenbildung von Sehnengewebe darzustellen. Ziel der Studie war es, die Elastizität von Achillessehnengewebe nach autologer mesenchymaler Stammzellapplikation unter Verwendung der Sonoelastographie zu untersuchen.

Material und Methodik: Die Achillessehne beider Hinterläufe wurde in neun Neuseeland Kaninchen vollständig durchtrennt. Anschließend wurden die Hinterläufe randomisiert drei Gruppen zugeteilt, wobei eine extrazelluläre Matrix mit Stammzellen (Gruppe 2, n=6) und ohne Stammzellen (Gruppe 3, n=6) verwendet wurde. In der Kontrollgruppe wurde eine Sham-Operation durchgeführt (Gruppe 1, n=6). Die Extraktion und Applikation der mesenchymalen Stammzellen erfolgte aus dem nuchalen Fettkörper zum gleichen Zeitpunkt wie die Achillessehnendurchtrennung, um die Untersuchung an einem autologen Sehnenregenerationsmodell zu untersuchen. Nach 8 Wochen wurden die Achillessehnen entnommen und die Elastizität mit einer hochauflösenden 6-15 MHz Matrix–Linear-Sonde untersucht. Für jede Sehne wurde eine 20 Sekunden farbkodierte Sonoelastographie-Sequenz aufgezeichnet und 10 Farbhistogramme untersucht. Definierte Regions of Interests (ROIs) wurden über den Sehnendefekt (n=3) und über angrenzendes vitales Sehnengewebe (n=3) gelegt. Für die semiquantitativen Auswertungen wurden 180 Einzelmessungen aufgezeichnet und ausgewertet.

Ergebnisse: In Gruppe 2 konnte für Achillessehnen mit beladener Matrix eine höhere Elastizität im Vergleich zu Achillessehnen mit unbeladener Matrix in Gruppe 3 gemessen werden ($p<0.001$; ANOVA). Hinsichtlich des Elastizitäts-Index (EI) von unbehandeltem Sehnengewebe (Gruppe 1) und Sehnengewebe mit beladener Matrix (Gruppe 2) konnte kein Unterschied gefunden werden ($p>0.05$). Für alle Einzelmessungen der verschiedenen Messzeitpunkte konnte kein signifikanter Unterschied festgestellt werden ($p>0.05$).

Schlussfolgerung: Unsere Ergebnisse zeigen, dass die Applikation von autologen mesenchymalen Stammzellen des Fettgewebes zu einer vollständigen Wiederherstellung der Elastizität des Sehnengewebes nach Achillessehnenverletzung führt. Außerdem konnte gezeigt werden, dass die

Sonoelastographie eine geeignete Methode ist, um die Regeneration der Elastizität nach Achillessehnenverletzung darzustellen und zu beurteilen.

Schlüsselwörter:
[Achillessehne], [adipose tissue-derived stem cells], [Elastizitaetsindex], [Sonoelastographie]

2. Summary

Purpose: Sonoelastography allows assessment of tissues' mechanical properties and has recently been used to demonstrate the effects of Achilles tendon injury. The aim of the current study was to evaluate an ultrasound approach to depict elastic recovery after stem cell application on injured Achilles tendon.

Materials and Methods: A rabbit achilles tendon injury model was used and randomized hindlimbs received either extracellular matrix with autologous adipose tissue-derived stem cells (group 2, n=6) or without (group 3, n=6). ASCs were harvested from the rabbits' nuchal fat body at the same time as the tendon injury operation. Untreated Achilles tendon (group 1, n=6) served as controls but underwent sham-operation. Specimens were harvested after 8 weeks and were longitudinal analyzed for elasticity using a high resolution 6-15 MHz matrix linear probe. For each tendon, real-time color-coded sonoelastography sequences of 20 seconds were recorded and ten color histogram frames were obtained. Defined regions of interest (ROIs) were placed on the defect (n=3) and on adjacent uninjured tendon tissue (n=3). In total, 180 measurements were obtained for semiquantitative analysis.

Results: Repeated measures ANOVA demonstrated a higher elasticity for stem cell seeded matrix (group 2) in comparison to the unseeded matrix (group 3) ($p<0.001$; ANOVA). No significant difference was found between the injured tendon tissue treated with stem cell seeded matrix (group 2) and uninjured Achilles tendons (group 1) ($p>0.05$). Moreover, no differences were found between the measurements at different time-points ($p>0.05$).

Conclusion: The current study indicates that autologous mesenchymal stem cell application successfully restores mechanical properties of injured tendon tissue. Furthermore, sonoelastography enables to monitor elasticity of injured Achilles tendon after stem cell application.

Keywords: **[Sonoelastography], [Achilles tendon], [Elasticity Index], [Adipose tissue-derived stem cells]**

3. Abbreviations

ASCs	Adipose tissue-derived stem cells
ANOVA	Analysis of variance
MHz	Mega Hertz
n	Number
ROI	Regions of interest
EI	Elasticity index
i.e.	Id est
ECM	Extracellular matrix
TSPC	Tendon stem/progenitor cell
Bgn	Biglycan
Fmod	Fibromodulin
VEGF	Vascular endothelial growth factor
IGF-1	Insulin-like-growth-factor 1
PDGF	Platelet derived growth factor
TGF-β	Transforming growth factor β
bFGF	Basic fibroblast growth factor
MSC	Mesenchymal stem cell
BMSC	Bone marrow-derived mesenchymal stem cell
ACL	Anterior crucial ligament
AT	Achilles tendon
BMMC	Bone marrow mononuclear cells
BMC	Whole bone marrow cells
PT	Patellar tendon
RC	Rotator cuff
SMSC	Synovial mesenchymal stem cells
SE	Sonoelastography
MRI	Magnetic resonance imaging
PBS	Phosphate bufferd saline
α-MEM	α-modification of Eagle’s medium
FBS	Fetal bovine serum
DAPI	4',6-diamidino-2-phenylindole

DMEM	Dulbecco's Modified Eagle's medium
DAB	3,3′-Diaminobenzidine
HRP	Horseradish peroxidase
BSA	Bovine serum albumin

4. Introduction

4.1 Achilles tendon

4.1.1 Extracellular matrix and stem cells in tendon tissue

The Achilles tendon is the strongest and sturdiest tendon in the human body[1] and serves as connective tissue which physically binds muscles (i.e. Musculus gastrocnemius) to skeletal structures[2] (i.e. Calcaneus). This facilitates enhancing joint stability and locomotion[3]. Tendon tissue has a multi-unit hierarchical organization of collagen molecules, fibrils, fibers, bundles, fascicles and tendon units, all running parallel to the tendon's longitudinal axis[3] designed to resist tensile load[4].

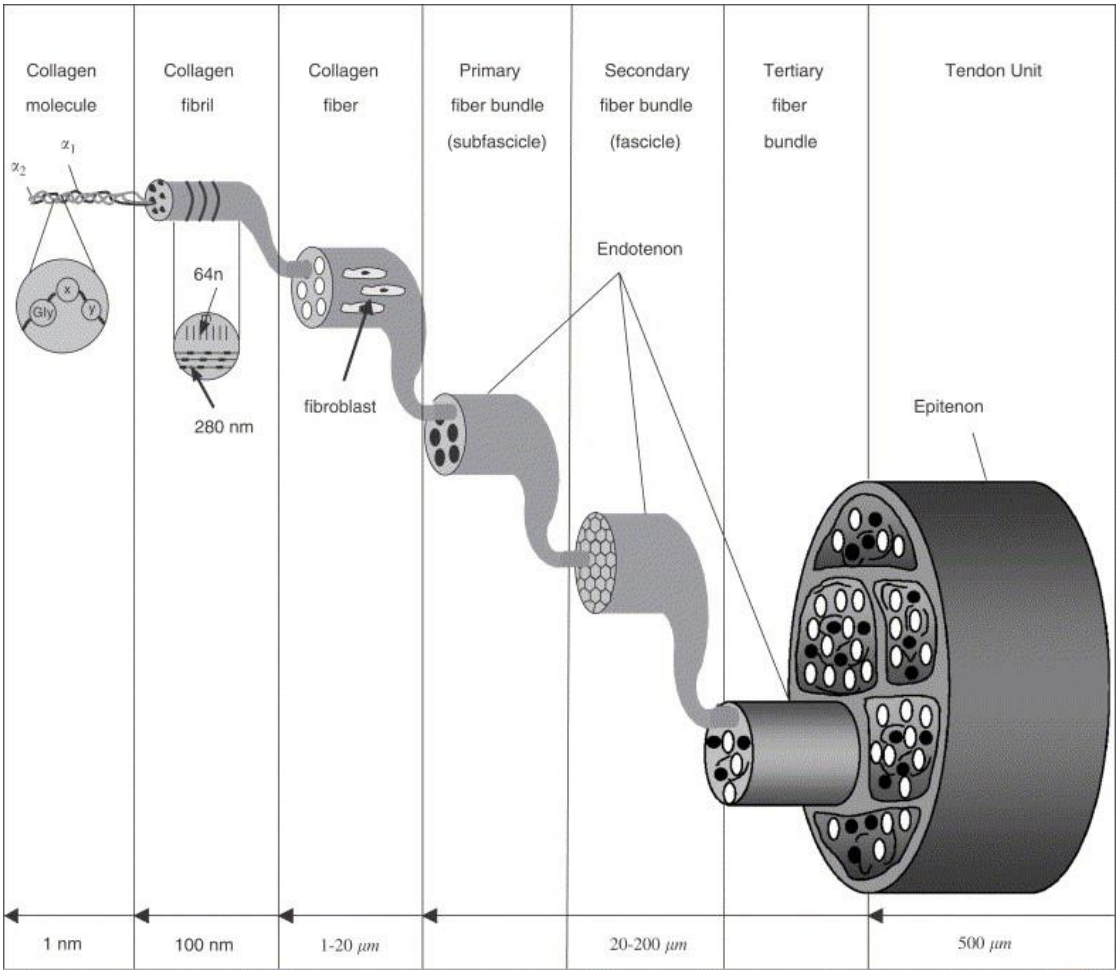

Figure 1: A drawing scheme of the multi-hierarchical structures of the tendon[3].

The structure of the extracellular matrix (ECM) molecules determines the physiological function and the mechanical strength of tendons[3]. The predominant molecule of tendon tissue is collagen I, which constitutes about 95% of the total collagen[5]. The overall content of cells is low[6] and primarily comprises of tenocytes and fibroblasts also referred to as tenoblasts. Both cell types are of mesenchymal origin and represent 90-95% of the cellular elements[4], in tendon tissue. The premature fibroblast differentiates into a tenocyte[7], featured with a very limited proliferation capacity[8]. Fibroblasts are responsible for synthesizing extracellular matrix proteins (e.g. collagen, fibronectin, proteoglycan), which aggregate to a collagen matrix. In addition, fibroblasts are responsible for remodeling the collagen matrix during tendon healing[3,8]. This comprises localized matrix formation and degradation which is crucial for tendon healing, adaptation to exercise, and tendon growth[8]. Recently, it has been shown, that tendon stem/progenitor cells (TSPCs) reside in ECM composed niche in tendon tissue and are controlled by biglycan (Bgn) and fibromodulin (Fmod). Moreover, isolated TSPCs could regenerate tendon-like tissues after extended expansion in vitro and transplantation in vivo[9]. However, repair mechanism of these stem cells is limited due to low cell number in tendon tissue.

Thus, limited healing of tendon tissue is emphasized by poor vascularization and nerve supply[10] as well as its low metabolic rate[11]. Additionally, Åström[12] et al. could demonstrate that mechanical loading but most important aging diminish the blood flow supplying the Achilles tendon.

4.1.2 Tendon regeneration and repair

A cascade of cellular and biochemical processes is initiated in order to restore tendons elasticity after injury. The initial stage involves tissue inflammation which attracts cells (e.g. inflammatory cells especially neutrophils, erythrocytes) from tissue adjacent to the side of injury[13]. Recruited fibroblasts maintain production of extracellular matrix during the proliferative phase. But new synthesized extracellular matrix is assembled in a random manner containing large number of cells and high amount of type III collagen[14,15]. Moreover, angiogenesis occurs during this stage[13]. Decrease of cellularity and type III

collagen starts 6 – 8 weeks after injury which is a characteristic feature of the remodeling stage. At the same time collagen I synthesis, as a crucial step for tensile strength[16], increases and provides longitudinal organized fibers along the lines of stress and a high rate of crosslinks which are responsible for tendon elasticity[15,17]. Additionally, elastic fibers with increased elastin deposition are observed[13].

During the different stages of tendon repair various growth factors activate and regulate the cellular response in a temporal and spatial manner. Vascular endothelial growth factor (VEGF) stimulates angiogenesis[15] and is produced at a maximum level after the inflammatory phase. In contrast, Insulin-like-growth-factor-1 (IGF-1) has been reported to be up-regulated highest at the inflammatory phase stimulating migration and proliferation of fibroblast and inflammatory cells[15,18]. Moreover, IGF-1 enhances collagen synthesis during the stage of remodeling accompanied by improved tendon stiffness[18]. In addition, platelet derived growth factor (PDGF) can facilitate IGF-1 expression during the inflammatory phase of tendon healing and is also involved in the remodeling process[18]. Thus, a lack of IGF-1 has been shown to be associated with an insufficient repair response[15]. Noteworthy, increased cell proliferation and synthesis of various ECM components especially collagen I during the remodeling phase has been reported for application of PDGF in a dose dependent manner[18]. In addition, TGF-β initiates cell migration and collagen production[19] and also effects the regulation of proteinases and fibronectin bindings[20]. But restored tendon tissue has thinner collagen fibrils which remain[21] and provides less mechanical properties than native tissue causing failure of tendons strength and eventual might lead to re-rupture[17].

4.1.3 Application of growth factors for Achilles tendon injury

Treatment options of Achilles tendon injury include nonsurgical treatment as immobilization in a cast or a functional brace[22]. Furthermore, surgical treatment exists and can decrease re-rupture rate[23] compared to conservative treatment protocol with immobilization. Recent studies suggest that growth factor application during tendon healing can enhance functional repair and might reduce time of regeneration. To date various growth factors are investigated for

possible application to improve tendon healing whereas VEGF, IGF-1, TGF-β, PDGF and bFGF are best characterized and known for their role in tendon tissue regeneration[18].

The delivery of one growth factor or even a mixture is challenging since the dosage of these factors is critical during each stage of the regeneration process. Furthermore, the limited half-life of growth factors and their small size restrict their retention for a prolonged time at applied site of tissue. These claims are supported by Zhang et al.[24] who showed that VEGF introduced exogenous to an injured tendon site can accelerate tensile strength just within the first 2 weeks postoperatively but no significant difference was seen after 4 weeks compared to the control group. Similar results were reported by treating patellar tendon defects in rabbits with IGF-1 and TGF-β1[25]. 2 weeks after administration a significant increase in ultimate stress, energy uptake, stiffness and force at failure were documented compared to the control group. Interestingly, 6 weeks after administration no significant difference was detected for all investigated parameters[25]. Thus, mesenchymal stem cells (MSCs) were suggested as an appropriate delivery method due to their engraftment at applied site and constant secretion of cytokines.

4.1.4 Stem cells for tendon tissue regeneration

Injury or degeneration of tissue of multicellular organisms can be restored by either scar formation or tissue regeneration. The capacity of regeneration is very limited to specific tissue (e.g. epidermis, intestinal mucosa[26]). In contrast, tendon as a self-contained tissue lacks the property of adequate regeneration due to low cell numbers.

Regenerative medicine is utilizing MSCs as a cell based tool since they show self-renewal and multi-lineage differentiation[27]. Furthermore, these cells have been shown to be hypo-immunogen due to the lack of the major histocompatibility complex-II molecular expression[28]. During the last decade different types of stem cells have been applied to tendon defects to investigate the potential for medical purposes in order to establish new experimental and clinical opportunities as seen in the Table 1. Regenerative medicine depends on stem cells that meet a number of qualities as 1. abundant appearance 2.

minimal invasive harvest 3. multi-linage differentiation and 4. safety and suitability for transplantation[29].

MSCs, as non-hematopoietic stem cells, have been primarily identified within the bone marrow stroma[30] and were considered the most promising source for medical tissue engineering application for a long time[31]. However, current studies showed that MSCs resides in almost all post-natal organs and tissues[32], including adipose tissue[33] as well as tendon[34]. In addition, Zuk et al.[33] demonstrated that the differentiation potential of ASCs is as effective as of other MSCs.

Table 1. Compilation of cell therapies for tendon healing

Cell type (Insertion)	Animal, Tendon	Major results	Author (Year)
BMSC (knitted scaffold)	Rabbit, AT	Improved biomechanics, histology (up to 4th week)	Ouyang[35], (2003)
BMSC (collagen gel)	Rabbit, PT	Improved biomechanics, histology No change in microstructure	Awad[36], (1999)
BMSC (fibrin)	Rabbit, AT	Improved biomechanics, histology (at 3 weeks only)	Chong[37], (2007)
BMMC (injected)	Human RC	All cases showed positive tendon integrity after 12 month, appears to be safe	Ellera Gomes[38], (2011)
BMSC (collagen sponge)	Rabbit PT	Improved biomechanics , histology	Juncosa-Melvin[39], (2006)
BMSC (collagen gel)	Rabbit AT	Improved biomechanics, histology	Young[40], (1998)
MSC (injection)	Rat, AT	Improved biomechanics, healing, enthesis	Nourissat[41], (2010)
BMC>MSC (injection)	Rat, AT	Improved biomechanics, increased Col I/III, VEGF and TGFbeta expression	Okamoto[42], (2010)
TDSC (fibrin glue)	Rat, PT	Improved biomechanics, histology	Ni[43], (2012)
SMSC (injection in bone tunnel)	Rat ACL	Accelerated tendon-bone healing, histology	Ju[44], (2008)

ACL, anterior crucial ligament; AT, Achilles tendon; BMMC, bone marrow mononuclear cells; BMC, whole bone marrow cells; BMSC, bone marrow-derived mesenchymal stem cells; MSC, mesenchymal stem cells; PT, patellar tendon; RC, rotator cuff; SMSC, synovial mesenchymal stem cells; TDSC, tendon-derived stem cells; TGF, transforming growth factor; VEGF, vascular endothelial growth factor; >, greater than;

4.1.5 ASCs for tendon tissue regeneration

The use of adipose tissue-derived stem cells, in particular, for tissue engineering has obvious advantage compared to other stem cells. The

application of embryonic stem cells is very restricted due to potential problems of cell regulation, ethical problems and different national laws whereas autologous mesenchymal stem cells can be used without hesitation as there are no ethical or immunological matters[33].

On proliferation rate ASCs' doubling time was 28 hours compared to BMSCs' 39 hours[45]. ASCs became popular for research and clinical application in first line because of equal efficiency regarding multi-lineage differentiation capacity and minimal invasive method of harvesting (local excision or suction-assisted liposuction[46]), low donor site morbidity[47] and the abundance of adipose tissue in adult humans. Thus, a high number of stem cells can be obtained. Furthermore, general or spinal anesthesia is often required[33] for bone marrow aspiration due to painful procedure. In addition, bone marrow aspiration is also known for yielding low numbers of MSCs (approximately 1 out of 10^5 adherent stromal cells)[30]. From this practical point of view an insufficient number of cells may necessitate an additional step of in vitro proliferation to generate a sufficient amount of cells for adequate clinical use. Additionally, liposuction might be more tolerated by patients than bone marrow aspiration due to its aesthetic effects.

Based on these properties ASCs became a valuable tool for tissue engineering and regenerative medicine. Several studies have been carried out to investigate effect of ASCs on tendon healing. As one promising step Uysal et al.[47] have enabled the differentiation of ASCs to tenocytes in vivo and furthermore demonstrated an improvement of tendons tensile strength after application of ASCs. In addition, tendons biomechanical properties enhance when combining MSCs with composite biomaterial scaffold[48]. Taken together, many studies concern themselves with the topic how new approaches using MSCs influence tendon healing and repair. These studies were mainly focused on established methods for assessing the grade of tendon healing like histology[35,40,49], immunhistochemistry[16,40,50] or biomechanical properties like tensile strength[47] or maximum stress[49].

The current study did not investigated biomechanical surrogate endpoints (e.g. tensile strength, maximum load or load to failure) since it has been extensively applied by various studies in the recent past[16,51]. This study centered on how

elasticity might serve as a surrogate marker for tendon healing linked to superior outcome since the elasticity of uninjured tendon tissue is accompanied by high energy uptake and the ability to deform.

4.2 Sonoelastography

Various animal models have been applied to investigate the role of MSCs on tendon regeneration. Interestingly, studies revealed that stem cell application can improve histological and biomechanical parameters but only in the first 6 weeks after tendon injury[37]. Moreover, at 12 weeks post-surgery, maximum strength is almost comparable to vital uninjured tendon tissue[40]. Macroscopical and histological scoring systems are already used to evaluate the quality of repaired tissue in tendon defect models[10]. However, a high number of animals have to be included in a study to investigate maximum force load and histology at various time points in a tendon injury model in order to ensure sufficient power for statistical analysis.

Moreover, histological and immunohistological examinations as well as biomechanical tests for evaluation of different parameters are either not feasible or not established for in vivo use during the healing process. Therefore, these diagnostic tools are inadequate for clinical use in daily routine to monitor the healing process of tendons after stem cell application.

Nevertheless, several techniques for in vivo evaluation of soft tissue, including tendon, are in clinical use. Magnetic resonance tomography, computer tomography and as the most widely-used ultrasound examination are tools for examination. However, the above mentioned diagnostic methods can only provide detailed information of tissue's morphology but not of biomechanical properties. However, biomechanical testing seems to be the gold standard for evaluating the efficiency of suture techniques or tendon strength, respectively[52,53]. Among tensile strength, maximum load or load to failure[16] elasticity, respectively stiffness[54], are biomechanical parameters of tendons. Thus, evaluation of tendon's elasticity might be a suitable marker to depict the healing process of a tendon regardless whether tendon tissue was treated conservatively, with suture or by regenerative methods like stem cell application.

Sonoelastography (SE), as a new and appropriate diagnostic tool for soft tissue, was first introduced in the early 1990s for in vitro use and subsequently evolved into in vivo use for imaging[55,56] to enable in vivo real-time measurement of tissue elasticity[57].

Sonoelastography is based on some basic principles allowing a qualitative determination of tissue elasticity. Manual palpation is one of the oldest medical examination methods[58]. Even nowadays it continues to be of great value in medicine, both practiced by professionals and as a technique for self-examination for lymph nodes, breasts, thyroid or Achilles tendon rupture. However, palpation is limited to superficial accessible structures and the interpretation is very limited due to a high subjectivity for information sensed by the fingers[59]. Like manual palpation sonoelastography detects elastic properties of tissue by comparing the grade of deformation between different types of tissue or between different regions of interest. Therefore the examiner performs strain with the ultrasound probe on structures amenable to compression. The maximum of displacement between two image points of the ultrasound B-mode in a determined time interval is computed by the instrument's software. The software generates a color-coded image, which displays certain displacements in a correspondent color which is superimposed on the B-mode image. The most common color definition depicts hard tissue as blue, intermediate as green and soft as red. The newest generation of sonoelastography device assigns a numerical value, known as elasticity index (EI) to each grade of color. This tool gives the examiner an opportunity to objectify elasticity in a more precise way. Constant and uniform compression and decompression must be applied to the tendon during sonoelastography in order to avoid misinterpretation and artifacts as well as to assure most exact values. Therefore modern software provides a visual indicator displayed on the monitor.

Recent studies using SE showed that elastic measurements of different types of tissue provide promising and useful result for diagnosis[59–62].

For tendon, in particular, Pedersen et al.[63] demonstrated that sonoelastography seemed to be as feasible as ultrasound and MRI assessing tendon alteration and furthermore was superior depicting subclinical alteration not detectable with conventional ultra sound. In addition, in a different study sonoelastography was able to distinguish between ruptured and healthy tendon by measuring

elasticity[64]. However, this study only used a grading of tendon elasticity (i.e. intermediate, hard, hardest) instead of EI. Moreover, every single tendon suffering a rupture exhibited heterogeneous structure during SE, whereas all healthy Achilles tendons had a homogeneous or relatively homogeneous structure. However, this study admits limitations due to high influence of the pressure of the probe on the tissue performed by the examiner. Taken together, the above mentioned findings support various studies which describe sonoelastography as a promising quantitative tool to characterize alteration in morphology or biomechanics induced by previous injury[65].

5. Aim of the study

The current study aimed to investigate whether:

i) ASCs are suitable to improve Achilles tendon elasticity when placed at the site of injury
ii) Sonoelastography is an appropriate and examiner independent tool to investigate elasticity of tendon tissue
iii) The content of Collagen I is changed by ASCs application
iv) ASCs are able to engraft at the side of application and survive at least 8 weeks
v) ASCs harvested from rabbit's nuchal fat body have multilineage pontential
vi) ASCs are able to change cell morphology and cell organization

6. Materials and methods

6.1 Materials

6.1.1 Substances

Povidone iodine	Sigma-Aldrich, St.Loise, MO, USA
Cefazolin	Pfizer, NYC, NY, USA
Blendzyme III	Roche Diagnostics, Basel, CH
PBS	Sigma-Aldrich, St.Loise, MO, USA
Hanks Balanced Salt Solution	Cellgro, Corning, NY, USA
α-modification of Eagle's medium	Cellgro, Corning, NY, USA 20%
FBS	PAN Biotech, Aidenbach, Germany
Penicillin- Streptomycin	Sigma-Aldrich, St.Louise, MO, USA
DAPI stock solution	Sigma-Aldrich, St.Louise, MO, USA
Buprenex	Reckitt Benckiser, Slough, UK
Meloxicam	Norbrook, Newry, North Ireland
Fentanyl citrate	Sandoz, Holzkirchen, Germany
Buthanasia solution	Virbac, Carros, France
Moist saline dressing	Sigma-Aldrich, St.Louise, MO, USA
Trypsin	PAN Biotech, Aidenbach, Germany
DMEM, low glucose with L-glutamine	Life Technologies, Carlsbad, CA, USA
Isobutyl-methylxanthine	Sigma-Aldrich, St.Louise, MO, USA
Dexamathasone	Sigma-Aldrich, St.Louise, MO, USA
Indomethacin	Sigma-Aldrich, St.Louise, MO, USA
Bovine panceas insuline	Sigma-Aldrich, St.Louise, MO, USA
Formalin	Sigma-Aldrich, St.Louise, MO, USA
Red Oil O stock	Sigma-Aldrich, St.Louise, MO, USA
Isopropanol 60%	Sigma-Aldrich, St.Louise, MO, USA
beta-glycerophosphate disodium salt hydrate	Sigma-Aldrich, St.Louise, MO, USA
L-ascorbic acid	Sigma-Aldrich, St.Louise, MO, USA
Alizarin Red S	Sigma-Aldrich, St.Louise, MO, USA

Ammonium hydroxide solution	Sigma-Aldrich, St.Louise, MO, USA
Ethanol 70%	Sigma-Aldrich, St.Louise, MO, USA
Ethanol 95%	Sigma-Aldrich, St.Louise, MO, USA
Xylene	Sigma-Aldrich, St.Louise, MO, USA
Paraplast Paraffin	Leica, Wetzlar, Germany
Hematoxylin Solution, Harris modified	Sigma-Aldrich, St.Louise, MO, USA
Ethanol 100%	Sigma-Aldrich, St.Louise, MO, USA
Lithium carbonate	Sigma-Aldrich, St.Louise, MO, USA
Eosin Y	Sigma-Aldrich, St.Louise, MO, USA
Phloxine B	Sigma-Aldrich, St.Louise, MO, USA
Acetic acid	Sigma-Aldrich, St.Louise, MO, USA
Cytoseal mounting media	Thomas Scientific, Swedesboro, NJ, USA
Mouse anti-rabbit monoclonal antibody-against Collagen-I	Abcam, Cambridge, England
Goat anti-mouse IgG H&L (HRP)	Abcam, Cambridge, England
Goat anti-mouse IgG H&L (Texas Red)	Abcam, Cambridge, England
Tris-EDTA buffer solution	Sigma-Aldrich, St.Louise, MO, USA
Tween 20	Sigma-Aldrich, St.Louise, MO, USA
Bovine serum albumin	Sigma-Aldrich, St.Louise, MO, USA
Hydrogen peroxide 30%	Sigma-Aldrich, St.Louise, MO, USA
Trisodium citrate dehydrate	Sigma-Aldrich, St.Louise, MO, USA
Triton X	Sigma-Aldrich, St.Louise, MO, USA
Sodium azide	Sigma-Aldrich, St.Louise, MO, USA
Gelatin from cold water fish skin	Sigma-Aldrich, St.Louise, MO, USA
3,3’-Diaminobenzidine	Sigma-Aldrich, St.Louise, MO, USA

6.1.2 Equipment

Autoclaving	Systec, Linden, Germany
Vicryl 4-0	Ethicon, Somerville, New Jersey
50 ml plastic pipette	Grainer bio-one, Kremsmünster, Austria
Shaker HS 501 digital	Ika Labortechnik, Staufen, Germany

50 ml plastic tube	Grainer bio-one, Kremsmünster, Austria
Centrifuge Multifuge 3S	Heraeus, Hanau, Germany
100µm Steriflip	Merck Millipore, Billerica, MA, USA
Collagen matrix (Puracol® Plus)	Medline Industries, IL, USA
Fume hood M18	Schulz Lufttechnik, Sprockhövel, Germany
Olympus BX 40	Shinjuku, Tokio, Japan
Polypropylene 2-0	Ethicon, Somerville, New Jersey
T75 culture flask	Sarstedt, Nürnbrecht, Germany
Incubator Hera Cell 240	Thermo Scientific, Waltham, MA, USA
Inverted microscope Wilovert S	Helmut Hund GmbH, Wetzlar, Germany
Refrigerator Liebherr medline	Liebherr, Bulle, Schweiz
6 well-plate cellstar	Grainer bio-one, Kremsmünster Austria
HM 400	Microm, Heidelberg
Slides	Engelbrecht GmbH, Edermünde, Germany
Microscope Axiovert	Carl Zeiss AG, Oberkochen, Germany
Camera Canon G7	Canon, Takio, Japan
Sonoelastographic device LOGIQ®E9	General Electrics, Fairfield, CT, USA
Multifrequency probe 6-15 MHz	General Electrics, Fairfield, CT, USA
Counting chamber Neubauer-improved	Paul Marienfeld GmbH, Lauda-Königshofen, Germany

6.1.3 Software

Real-time sonoelastography software	General Electrics, Fairfield, CT, USA
GraphPad Prism 5 for Windows	GraphPad Software Inc., La Jolla, CA, USA

6.2 Methods

6.2.1 Preparation of the fat body

A total of nine male New Zealand white rabbits weighing 3.5±0.5 kg were used to evaluate if sonoelastography is able to depict elastic recovery after autologous adipose-derived stem cell application on injured Achilles tendon following the guidelines of Veterinary Medicine & Surgery at MD Anderson Cancer Center and US National Institutes of Health. The study was approved by the IACUC of MD Anderson Cancer Center Houston. All the rabbits were aged 14 to 16 weeks and were randomly assigned to either a control group without injury or a group treated with ASCs seeded collagen matrix or treated with unseeded collagen matrix. Equipment for all operations was sterilized by autoclaving at MD Anderson facility. All animals were anaesthetized by administration of isoflurane received by mask. Anesthesia was monitored by respiratory rate and heart rate, response to noxious stimulus, spontaneous movement, pedal reflex, oxygen saturation and body temperature. Each rabbit was placed in prone position for harvesting the nuchal fat body. The hair in the field of operation was shaved and the skin was surgically prepared using povidone iodine for disinfection. Subsequently, the animal was transferred to a heated surgery table and the nuchal region was covered with a sterile surgical drape. A small incision of 3 cm with a scalpel no. 15 was made to approach the rabbit's nuchal fat body (Figure 2), which was excised bilaterally and transferred into a sterile container for stem cell harvesting. The mean weight of the fat bodies was 15±2.4 grams. The subcutaneous layer and the skin were closed by continuous suture technique with Vicryl 4-0. Every step was performed by using aseptic techniques. All animals received perioperative doses of prophylactic antibiotics (Cefazolin 15mg/kg, i.v.).

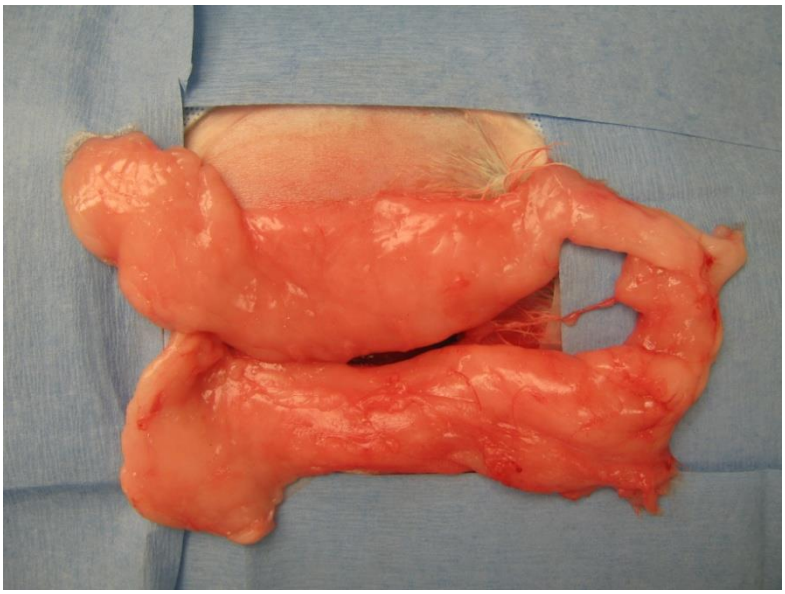

Figure 2: Nuchal adipose fat body that was used to harvest adipose tissue derived mesenchymal stem cells after surgical preparation.

6.2.2 Stem cell isolation

Nuchal fat tissue was extensively washed in PBS after harvesting and subsequently minced in pieces less than 1mm³. Subsequently, the minced tissue was incubated in PBS containing Blendzyme III (2U/mL) for 30 minutes at 37°C on a shaker at 100 rpm. After digestion, the suspension was disaggregated by pipetting 5 times under sterile conditions and was transferred into a 50 ml plastic tube followed by centrifugation at 450g for 10 minutes (Figure 3). The supernatant was discarded and cells were washed twice with PBS. Afterwards, cells were vacuum filtered through a 100 µm Steriflip. The filtered cell suspension was then centrifuged at 450g for 10 minutes. The supernatant containing adipocytes and debris was discarded and the pelleted cells were washed twice with 40 ml Hanks Balanced Salt Solution. The pellet was resuspended in PBS for immediate application or for further in vitro experiments in alpha-MEM supplemented with 20% fetal bovine serum (FBS), 100 U/ml penicillin and 100 µg/ml streptomycin. For immediate application cell number was determined using a Neubauer chamber. Subsequently, the suspension with the ASCs was seeded on a collagen matrix with $1x10^6$ stem cells in 200µl PBS after labeling with DAPI. Except for digestion and

centrifugation all steps were performed under a fume hood to remain sterile conditions.

Table 2. Preparation of 500 ml growth medium

Reagents	Amount
FBS	100 ml
Glutamine	14,61 g (2 mM)
Streptomycin	50 mg
Penicillin	50000 U
alpha MEM	Up to 500 ml

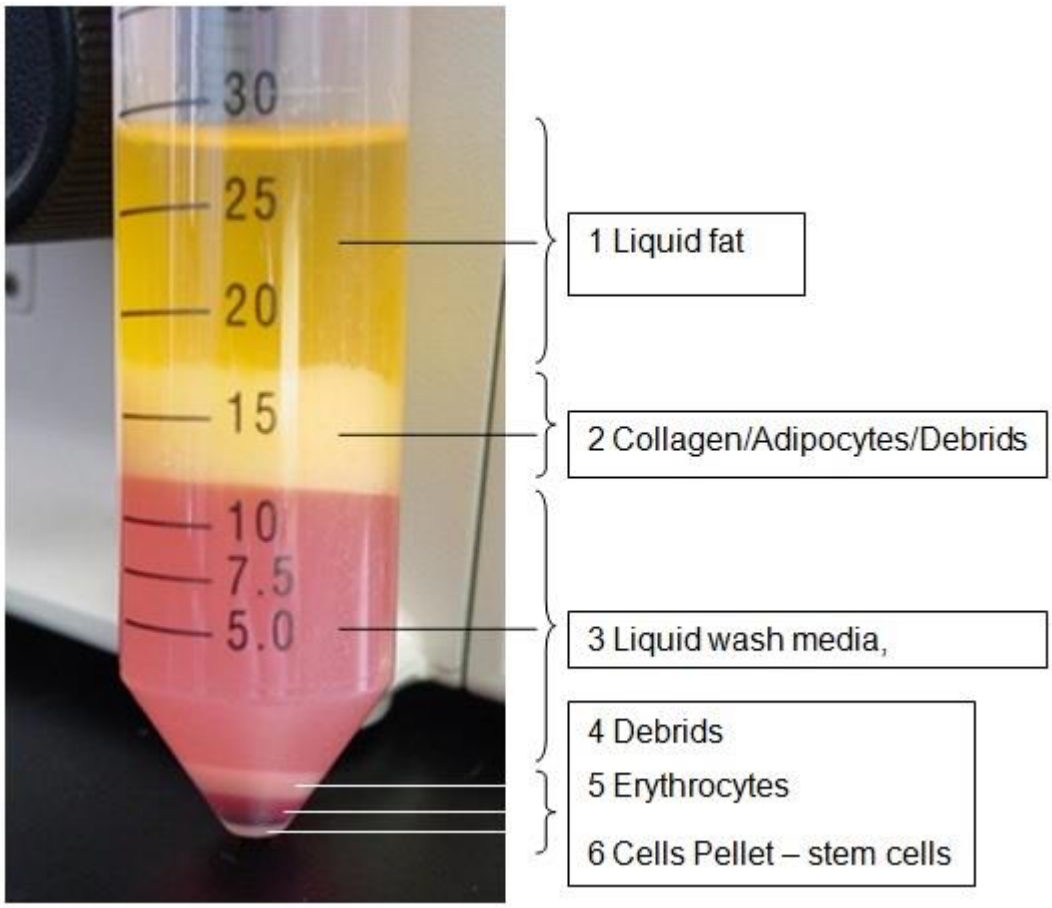

Figure 3: 50 ml plastic tube after first centrifugation with 450 g for 10 minutes, fraction 6 shows the stem cell pellet

6.2.3 DAPI labeling of ASCs and fluorescence microscopy

Freshly isolated ASCs from the rabbit's nuchal fat body were labeled with DAPI before seeded onto the collagen matrix. DAPI stock solution (Table 3) was diluted to final concentration of 50µg/ml in PBS and ASCs were incubated for 30 minutes at 37°C. Afterwards, cells were centrifuged at 500g for 5 minutes, and resuspended in PBS to further seed onto the matrix. Final DAPI concentration was revealed by testing ascending concentration without inducing apoptosis in previous tests.

For fluorescence microscopy 8 µm-thick sections were prepared from each tendon and 3 sections were microscoped to test for the presence of ASCs. Tissue sections were microscoped using 358 nm wavelength and emission filter of 461 nm. All stained slides for fluorescence microscopy were analyzed using a Olympus BX 40 microscope equipped with a Canon G7 high-resolution digital camera adapter for image acquisition.

Table 3. Preparation of 100 ml DAPI working solution

Reagents	Amount
DAPI stock solution	5000 µg
PBS	Up to 100 ml

6.2.4 Preparation of the Achilles tendon

The hair of both hind limbs was shaved and the skin was disinfected with povidone iodine using aseptic techniques. Both hind limbs were covered with a steril surgical drape. Under aseptic conditions, a 3 cm small sharp skin incision was made with a scalpel no. 15 laterally to the Achilles tendon and the tendon was exposed. The peritendon was opened and the tendons of the musculus plantaris, soleus and gastrocnemius were identified and segmented (Figure 4a). Only the gastrocnemius tendon was transected with a scalpel blade perpendicular to the collagen fibers 3 cm above the tendon insertion of the calcaneus. A gap of 10 mm was created on each limb and the defect randomly

received either a collagen matrix (Puracol® Plus) with $1x10^6$ stem cells (group 2, n=6 tendons) suspended in 200µl PBS or without stem cells (group 3, n=6 tendons). Collagen matrix was sutured in place using a modified Kessler pattern with 2-0 polypropylene. Control animals received no injury (group 1, n=6 tendons) but were sham operated. Skin was closed by suture using 4-0 Vicryl. The leg was bandaged and postoperative analgesia were accomplished with Buprenex 0.5-2.5 mg/kg s.c./i.m. and Meloxicam (0.2 mg/kg, i.m. first day followed by 0.1 mg/kg once per day) or Fentanyl citrate. The rabbits were not immobilized postoperatively and were fed ad libitum. In a preliminary study we established the operation technique which provides enough movement of the animals to access food and water due to intact soleus and plantaris tendon. During the postoperative time, clinical parameters including activity, infection, bleeding, appetite and wound dehiscence were evaluated daily. All nine animals were anesthetized by isoflurane and sacrificed by an overdose of Buthanasia solution 8 weeks after tendon surgery to remove the whole tendons for sonoelastographical examination (Figure 4b). For harvesting the specimens, the calcaneus with Achilles tendon was displaced and the gastrocnemius muscle was transected. Tendons were packed in moist saline dressings, frozen and stored at -20°C. For sonoelastography tendon were slowly thawed over night in a refrigerator at 4°. One hour prior to the experiment tendons were equilibrate at room temperature and kept moist by saline solution. Tendons were fixed by pins on a cork board without tension. All sonoelastographic measurements were performed on the same day.

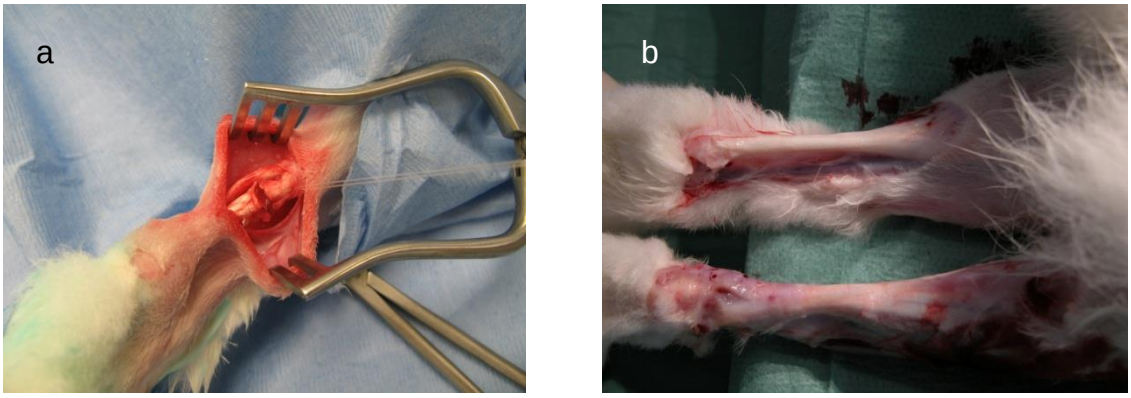

Figure 4: After gastrocnemius tendon dissection insertion of the collagen matrix and fixation with a modified Kessler suture technique (a). Scar formation of Achilles tendon after 8 weeks of gastrocnemius tendon dissection (b).

6.2.5 Expansion and subculturing of ASCs

The cell pellet was resuspended after isolation in complete growth medium consisting of alpha-MEM, 20 % FBS, 2 mM L-glutamine, 100 U/ml penicillin and 100 µg/ml streptomycin. Plastic adherent ASCs were grown in appropriate cell culture flasks and placed in an incubator at 37 °C in a humidified atmosphere containing 5 % CO2. Daily washings on the first 2 days removed nonattached cells. Growth medium was exchange twice a week until 90 % confluency. Cell culture was examined daily under an inverted microscope. After reaching 90% confluency the medium was discarded and cells were washed twice with PBS. Trypsin was added (1ml for a T75 flask) and incubated for 3 minutes at 37°C in a humidified atmosphere containing 5 % CO2. Subsequently, the effect of trypsin was neutralized by adding growth medium. Cells were centrifuged at 500g for 5 minutes, resuspended in growth medium and splitted 1:3 for subculturing.

Table 4. Preparation of 500 ml growth medium

Reagents	Amount
FBS	100 ml
Glutamine	14,61 g (2 mM)
Streptomycin	50 mg
Penicillin	50000 U
alpha MEM	Up to 500 ml

6.2.6 Adipogenic differentiation of ASCs

Plastic adherent ASCs were washed twice with PBS and trypsinized by 0.25% trypsin. Cells were seeded into 6 well-plates at a concentration of $1.5x10^4$ cells per cm^2 and adipogenic differentiation was induced by differentiation medium consisting of growth media (Table 4) with 0.5 mM Isobutyl-methylxanthine, 10 µM bovine insulin, 1 µM dexamathasone and 200 µM indomethacin (Table 5).The medium was changed every 3 days whereas only ASCs in passage below 5 were used for adipogenic assay to ensure efficient differentiation. ASCs were exposed to adipogenic induction media for a period of 14 days.

Table 5. Preperation of 100 ml adipogenic differentiation medium

Reagents	Amount
Dexamethasone	39,2 µg (1 µM)
Isobutyl-methylxanthine	11,21 mg (0,5 mM)
Bovine insulin	5,78 mg (10 µM)
Indomethacin	7,16 mg (200 µM)
Growth medium	Up to 100 ml

Adipogenic transdifferentiation was detected by Oil Red O staining which detects intracellular oil droplets, triglycerides respectively. Oil Red O working solution was prepared by 6 parts of Oil Red O working solution and 4 parts of distilled water (Table 6). Induction medium was discarded and cells were fixed with 4% formalin for 5 minutes at room temperature. Formalin was discarded and fresh formalin was added for an incubation of 60 minutes. Afterwards formalin was removed and cells were washed with 60% isopropanol. Oil Red O working solution was added and incubated for 10 minutes followed by washing four times with distilled water. Finally 4 ml of distilled water was added to prevent the cells from drying.

Table 6. Preperation of 100 ml Oil Red O Working Solution

Reagents	Amount
Oil Red O stock	60 ml (0,21 g Oil Red O)
dH2O	40 ml

6.2.7 Osteogenic differention of ASCs

Plastic adherent ASCs were washed twice with PBS and trypsinized by 0.25% trypsin. Cells were seeded into 6 well-plates at a concentration of $1.0x10^4$ cells per cm^2 and osteogenic differentiation was induced by differentiation medium consisting of Growth media (Table 4) with 10 mM beta-glycerophosphate disodium salt hydrate , 50 µM L-ascorbic acid, and 100 nM dexamethasone

(Table 7). The medium was changed every 3 days whereas only ASCs in passage below 5 were used for osteogenic assay to ensure efficient differentiation. ASCs were exposed to osteogenic induction media for a period of 14 days.

Table 7. Preparation of 100 ml osteogenic differentiation medium

Reagents	Amount
Dexamethasone	3,92 µg (100nM)
L-ascorbic acid	0,881 mg (50 µM)
Beta-glycerophosphate disodium salt hydrate	0,461 g (10mM)
Growth medium	Up to 100 ml

Osteogenic transdifferentiation was detected by Alizarin Red S staining which detects osteocytes' calcium deposits. Alizarin Red solution was prepared of 2g Alizarin Red with 100 ml of distilled water (Table 8). The pH-value was adjusted to 4,1-4,3 with ammonium hydroxide solution. Induction medium was discarded and cells were fixed by incubating in iced cold 70% ethanol for 60 minutes at room temperature. Ethanol was discarded and cells were rinsed twice for 5 minutes with distilled water. Afterwards 5 ml of the Alizarin Red S solution was added and incubated for 30 minutes at room temperature. Alizarin Red S solution was removed and each well was washed four times with distilled water. Finally 4 ml of distilled water was added to prevent the cells from drying.

Table 8. Preparation of 100 ml Alizarin Red S Solution

Reagents	Amount
Alizarin Red S	2 g
dH2O	Up to 100 (50 µM)
ammonium hydroxide solution	up to pH 4,1-4,3

6.2.8 Histology

After sonoelastography tendon tissue was immediately washed extensively with PBS to removed remaining ultrasound gel and placed in 4% formalin for 24 hours followed by ascending ethanol series starting at 70% for 60 minutes followed by 95% ethanol for 60 minutes, first 100% ethanol for 60 minutes, second 100% ethanol for 90 minutes, third 100% ethanol for 90 minutes and fourth 100% ethanol for 120 minutes. Next the tendons were processed twice with xylene as clearing agent for 60 minutes each. Ethanol and xylene were replaced with fresh reagents after every use. Fixed tissue specimens were embedded in paraffin wax for 60 minutes at 58°C. 3 µm serial sectioning of paraffin-embedded specimen blocks was performed with a HM 400. For histology 3 µm slides were deparaffinized by 2 changes of xylene for 10 minutes each and rehydrated in 2 changes of absolute ethanol for 5 minutes each, 95% ethanol for 2 minutes and 70% ethanol for 2 minutes followed by rinsing in distilled water for 5 minutes.

Tissue sections were stained in hematoxylin (Table 13) solution for 6 minutes and rinsed for 20 minutes in tap water. Afterwards, slides were decolorized in acid alcohol (Table 12) for 1 second followed by rinsing again for 5 minutes in tap water. Next specimens were immersed in lithium carbonate (Table 14) for 3 seconds, rinsed in tap water for 5 minutes and counterstained in eosin solution (Table 9) for 15 seconds. Stained specimens were dehydrated with 2 changes of 95% ethanol for 3 minutes and 2 changes of 100% ethanol for 3 minutes. Specimens were cleared in 2 changes of xylene for 5 minutes each. Ethanol and xylene was discarded after each use. Finally the stained specimens were mounted with cytoseal in a fume hood.

Table 9. Preparation of working solution eosin

Reagents	Amount
Eosin stock	100 ml
Phloxine B stock solution	10 ml
95% ethanol	780 ml
Acetic acid	4 ml

Table 10. Preparation of eosin stock solution

Reagents	Amount
Eosin Y	1 g
dH20	100 ml

Table 11. Preparation of phloxine B stock solution

Reagents	Amount
Phloxine B	1 g
dH2O	100 ml

Table 12. Preparation of 0,25% working solution acid alcohol

Reagents	Amount
95% ethanol	2578 ml
dH2O	950 ml
HCL	9 ml

Table 13. Preparation of Working solution hematoxylin

Reagents	Amount
Hematoxylin Solution, Harris modified	1 L

Table 14. Preparation of working solution lithium carbonate

Reagents	Amount
Lithium carbonate	47 g
dH2O	3500 ml

A series of 3 µm-thick sections were utilized for immunohistochemical staining. A mouse anti-rabbit monoclonal antibody against collagen I was used to detect the expression of collagen I in Achilles tendon tissue. For pretreatment heat-induced retrieval was conducted to break the methylene bridges, formed during fixation, to expose antigenic sites in order to allow the antibodies to bind. Therefore antigen retrieval buffer (Tris-EDTA) was added to a pressure cooker

that was placed on a hotplate. Once boiling, the slides, placed in a metal rack, were transferred to the pressure cooker. Lid was secured and as soon as full pressure was reached, slides were processed for further 3 minutes. When time was elapsed pressure cooker was placed in an empty sink and pressure was released while cooling down in running tap water. Once depressurized lid was opened cold running water was applied into the pressure cooker for 10 minutes.

Next, pretreated slides underwent the staining procedure. First every slide was rinsed with 2 changes of PBS-Tween 20 (Table 17) for 2 minutes and then incubated in universal blocking buffer (Table 16) for 120 minutes at room temperature. Slides were rinsed in PBS Tween-20 before applying the mouse anti-rabbit monoclonal antibodies against collagen I diluted 1/200 in antibody dilution buffer (Table 18) for incubation at 4°C overnight. Next, slides were again rinsed with PBS-Tween 20 and incubated in 0.3% peroxidase in PBS blocking solution (Table 15) for 15 minutes at room temperature. After rinsing with PBS-Tween 20, slides were incubated with the secondary goat anti mouse HRP conjugated antibody diluted 1/500 in antibody dilution buffer for 1 hour at room temperature. Working solution of DAB was applied to tissue section for 10 minutes and monitored for chromogenic reaction. Slides were washed twice with distilled water for 2 minutes each followed by dehydration, clearing and mounting as described above. All stained slides were analyzed using an Axiovert microscope equipped with a Canon G7 high-resolution digital camera for image acquisition. For fluorescence histology a Texas Red conjugated goat anti-mouse antibody was used as secondary antibody. All steps of staining, except of the application of DAB, were performed in the same way. For analyzing the slides microscopy was performed in the dark using 586nm wavelength and an emission filter of 605 nm.

Table 15. Preparation of peroxidase blocking solution

Reagents	Amount
30% Hydrogen peroxide	10 ml
PBS	990 ml

Table 16. Preparation of 100 ml universal blocking buffer

Reagents	Amount
BSA	1 ml
Cold fish skin gelatin	0,1 ml
Triton X-100	0,5 ml
Sodium azide	0,05 ml
PBS	up to 100 ml

Table 17. Preparation of PBS-Tween 20

Reagents	Amount
PBS	95 ml
Tween 20	5 ml

Table 18. Preparation of 100 ml antibody dilution buffer

Reagents	Amount
BSA	1 ml
PBS	99 ml

6.2.9 Sonoelastography

The experimental set-up included a LOGIQ®E9 (General Electrics) (Figure 5, 6) using a linear high resolution multifrequency probe from 6-15 MHz (Figure 7). The same conditions of brightness, contrast, intensity, color scale and frequency were used in all examinations. All measurements were performed by one experienced examiner (more than 5000 examinations per year). First an examination with the fundamental B-scan was performed in the longitudinal plane of the Achilles tendon to localize a potential irregularity of the tendon after the earlier disruption or as the development of the repair mechanism. Then the color coded ultrasound elastography was performed for whole tendon tissue up to a distance from 4 cm in the longitudinal plane and 5 mm in the axial plane. The probe was perpendicular to the tendon in order to avoid anisotropy. The aim was to find changes of the color coded evaluated tissue elasticitiy in relation to surrounding normal tissue (red colour), tissue with good elasticity (yellow colour), particularly fibrosis (green colour), or a scar (blue colour). For each tendon real-time color-coded sonoelastography sequences of 20 seconds were

recorded. A quality marker was used to evaluate the best compression mode. Only sequences with the highest image quality with five green points were used for an appositional evaluation by a quantification mode (Q-analysis) integrated in the ultrasound machine workstation. Ten color histogram frames were obtained for each tendon at ten randomly chosen time-points. Regions of interest (ROIs) were placed on the defect (n=3) and on adjacent uninjured tendon tissue. Real-time sonoelastography software calculated tendon's elasticity in the region of interest by depicting certain local tissue displacement during a time shift in a certain color. A quantified value was assigned to each color, which serves as the elasticity index (EI) and ranges from 0.0 to 6.0. Higher values represent higher stiffness and are visualized by a dominant blue color. This provides more objective information about the elasticity. Elasticity of the specimen was reconstructed by calculation of tissue displacement using the elastogram as a color overlay superimposed on the B-mode ultrasound image. A visual indicator on the screen displayed ongoing tissue compression to assure correct technique of compression and decompression applied to the tendon. All tendons were covered with ultrasound gel for a longitudinal examination (Figure 8).

A total of 180 measurements were obtained and mean intensity of color histograms were computed by a novel customized GE software. Ten time-point measurements ensured that EI was not affected by compression variances caused by the examiner. All of these images were recorded on a hard disk and used for statistical evaluation.

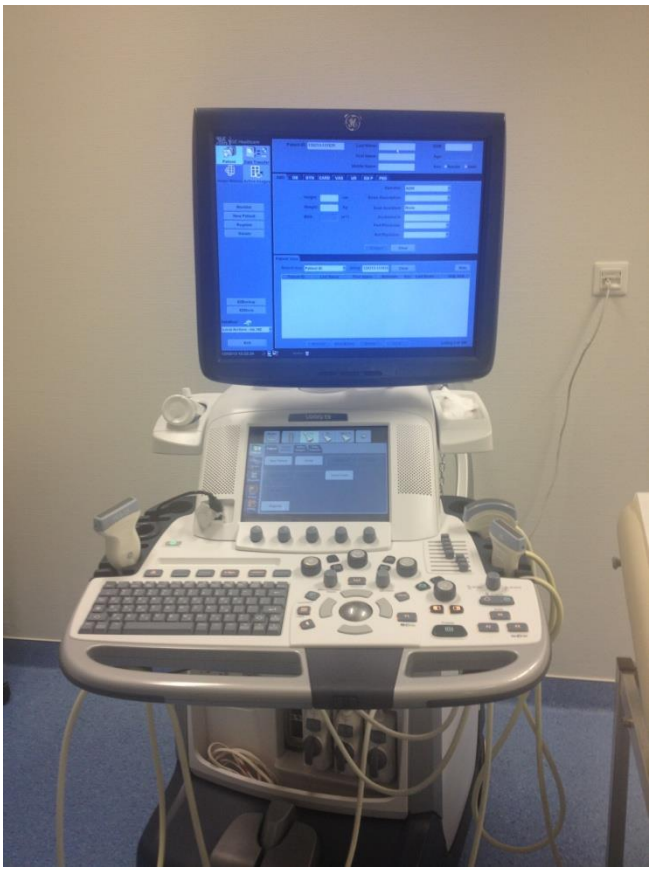

Figure 5: LOGIQ®E9 (General Electrics)

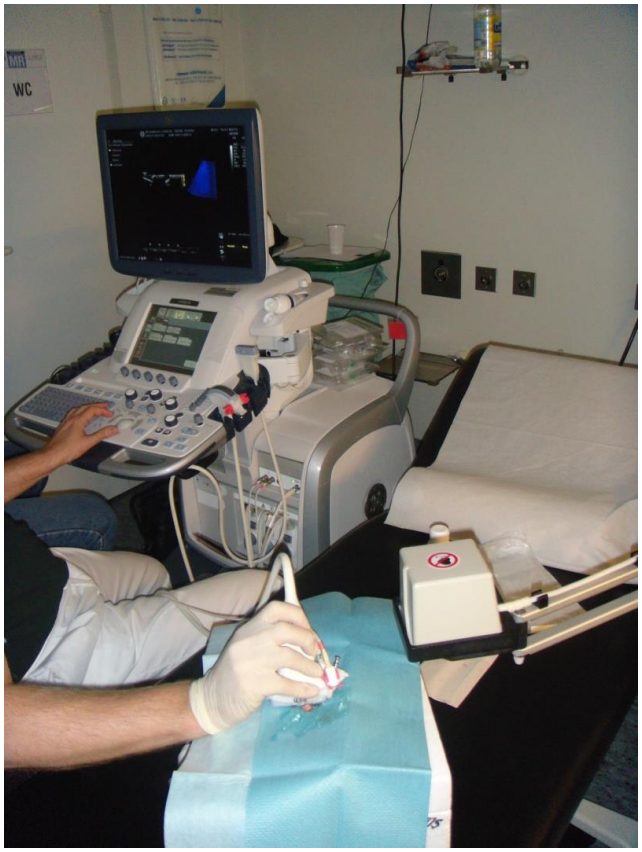

Figure 6: Experimental set up including a LOGIQ®E9

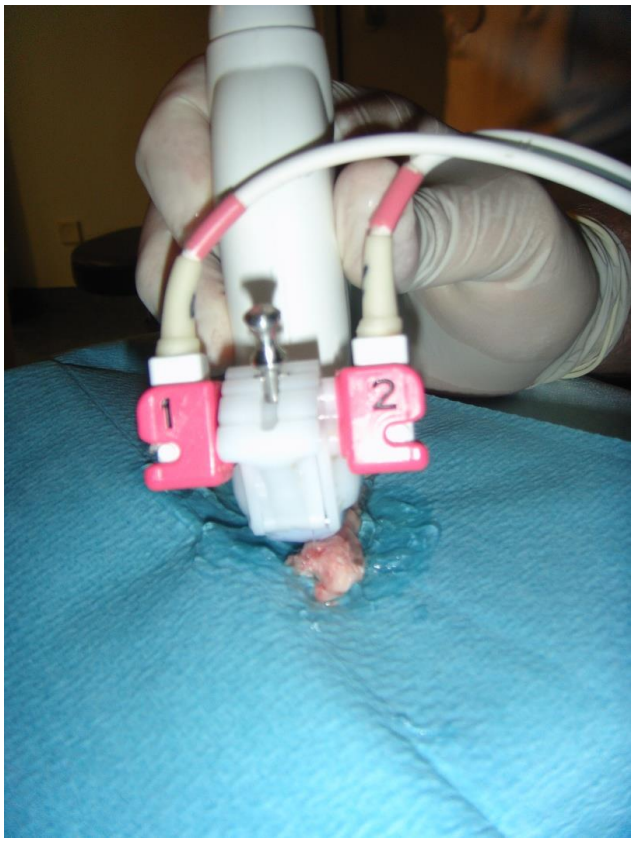

Figure 7: Linear high resolution multifrequency probe from 6-15 MHz during examination

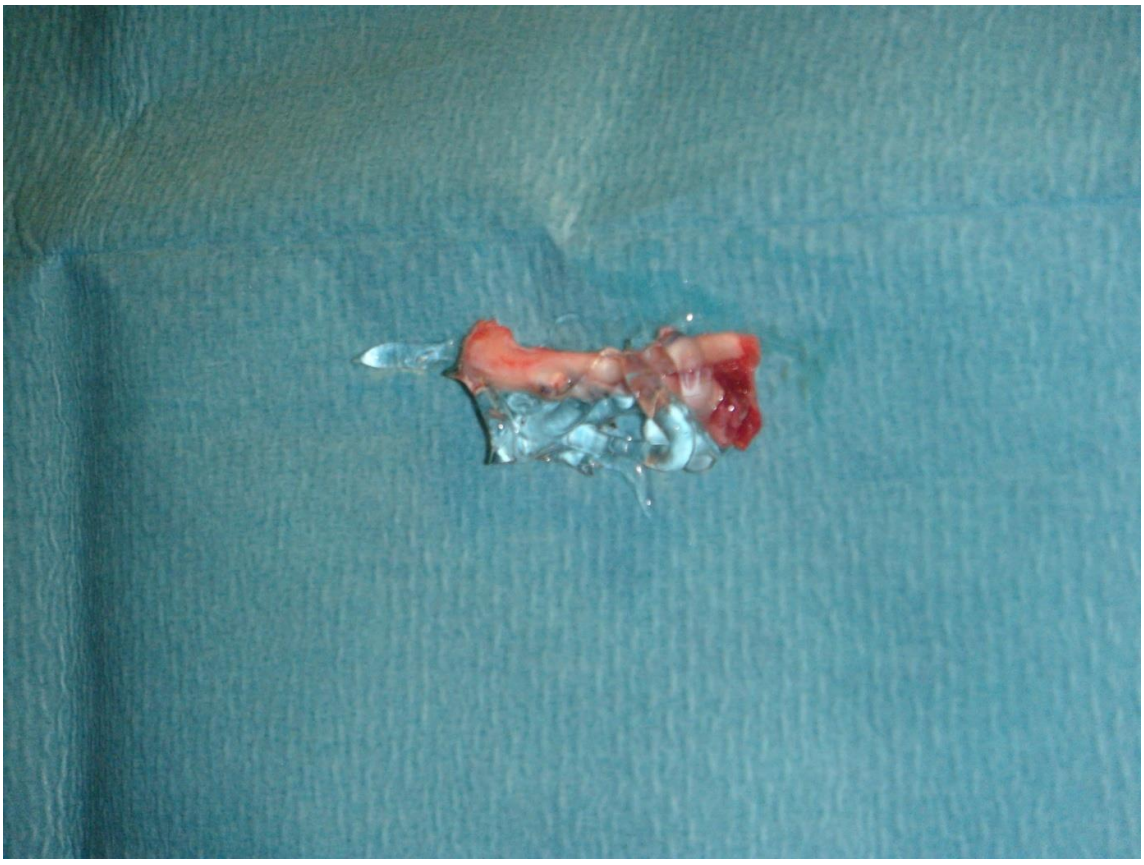

Figure 8: Achilles tendon covered in ultrasound gel before examination

6.2.10 Statistical analyses

Statistics were calculated using GraphPad Prism 5 for Windows. Results are shown as means ± standard deviation. All data sets of metric variables were checked for Gaussian distribution (Kolmogorov-Smirnov test, alpha = 5 %). Continuous variables were compared by means of one-way ANOVA with Scheffe post hoc correction. Differences between the ten time-points for sonoelastographic measurements were examined by repeated measures ANOVA with a Greenhouse-Geisser correction since assumption of sphericity had been violated (Mauchly's Test of Sphericity $p < 0.0001$). Values at $p < 0.05$ were considered as statistically significant.

7. Results

7.1 ASC preparation and injection

Nuchal adipose tissue was successfully harvested from all animals followed by enzymatic digestion in order to extract mesenchymal stem cells. Mean weight of harvested nuchal fat tissue was 15 g ± 2.4 g. Skin incisions healed without complications or defects in all rabbits. All cells were processed as described above and total yield of freshly isolated cells ranged from 27.5 x 10^6 to 31.3 x10^6 cells with a cell viability of 91%±3.2%. During the postoperative time, clinical parameters including activity, infection, bleeding, appetite and wound dehiscence were observed without any complications or irregularities.

7.2 Transdifferentiation of ASCs

7.2.1 Adipogenesis

Adipose derived stem cells of rabbits nuchal fat tissue were treated with adipogenic differentiation medium and showed differentiation into adipocytes. Differentiated stem cells contained Oil Red O-positive lipid vacuoles (triglyceride) clustered within cytoplasma after 14 days of adipogenesis (Figure 9a). A negative control, receiving growth medium instead of adipogenic differentiation medium, did not show any Oil Red O positive lipid vacuoles (Figure 9b).

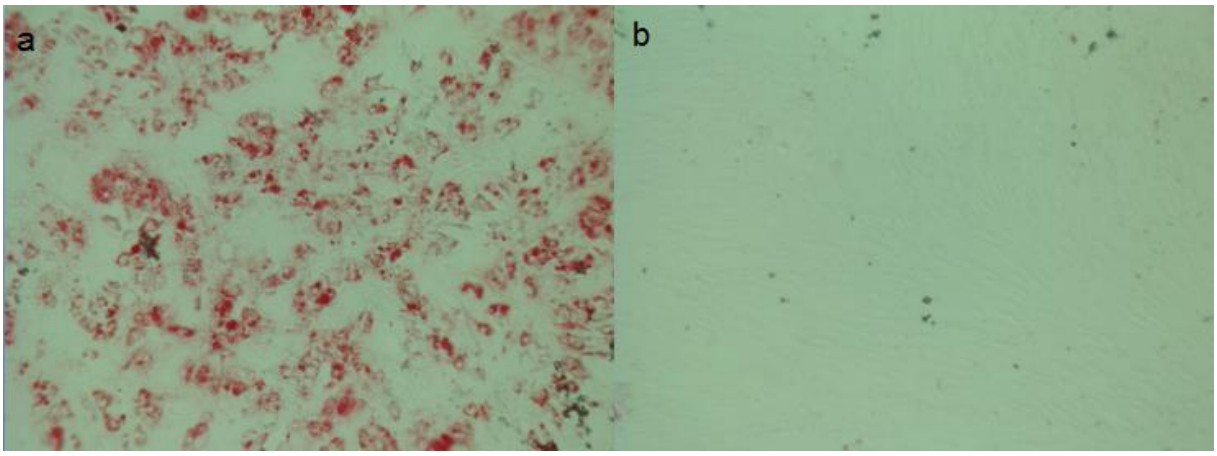

Figure 9: (a) Adipogenic differentiation of ASCs after 14 days of incubation with adipogenic differentiation medium, stained with Oil Red O. (b) negative control of ASCs incubated with growth medium for 14 days, also stained with Oil Red O

7.2.2 Osteogenesis

Treatment of adipose derived stem cells from the nuchal fat tissue with osteogenic differentiation medium resulted in a differentiation of ASCs into osteocytes. Successfully differentiated stem cells produced Alizarin Red S-positive nodules of mineralized calcium phosphate matrix above the cell monolayer after 14 days of osteogenesis (Figure 10a). A negative control, receiving growth medium instead of osteogenic differentiation medium, did not show any Alizarin Red S-positive nodules (Figure 10b).

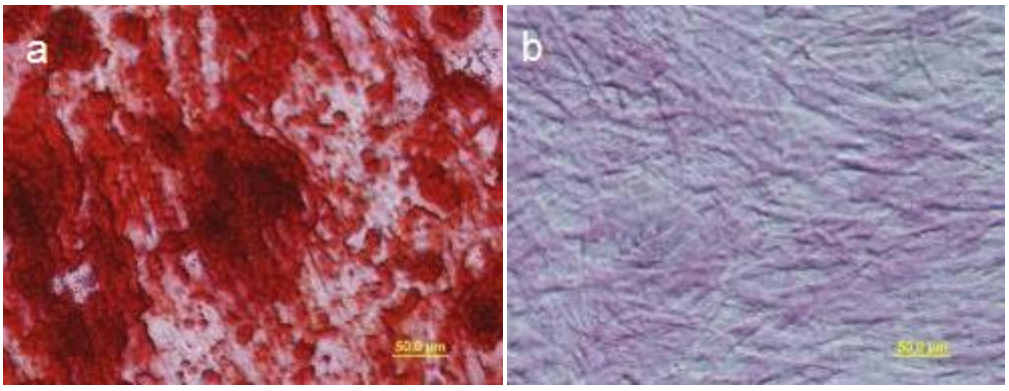

Figure 10: (a) Osteogenic differentiation of ASCs after 14 days of incubation with osteogenic differentiation medium, stained with Alizarin Red, (b) negative control of ASCs incubated with growth medium for 14 days, also stained with Alizarin Red

7.3 Effects of ASCs on tendon's elasticity

Real time sonoelastography was performed in order to characterize the elasticity of Achilles tendons. Elasticity index (EI) was calculated from regions of interest, which were placed on injured (n=3) and non-injured (n=3) tissue on each tendon. The mean EI from Achilles tendons without injury (group 1), injured achilles tendons with ASC seeded matrix (group 2) and injured tendons with unseeded matrix (group 3) were compared to evaluate the effect of applied stem cells.

Post hoc tests using the Scheffe correction revealed a higher elasticity, measured by EI for the injured tendon tissue treated with ASC seeded matrix (group 2, Figure 11a) in comparison to the unseeded matrix (group 3, Figure 11b) (0.73±0.26 and 4.02±1.33, respectively; $p<0.01$; Figure 11c).

In addition, no difference was found between the injured tendon tissue treated with ASC seeded matrix (group 2) and the uninjured Achilles tendons (group 1) (0.73±0.26 and 1.05±0.40, respectively; $p>0.05$).

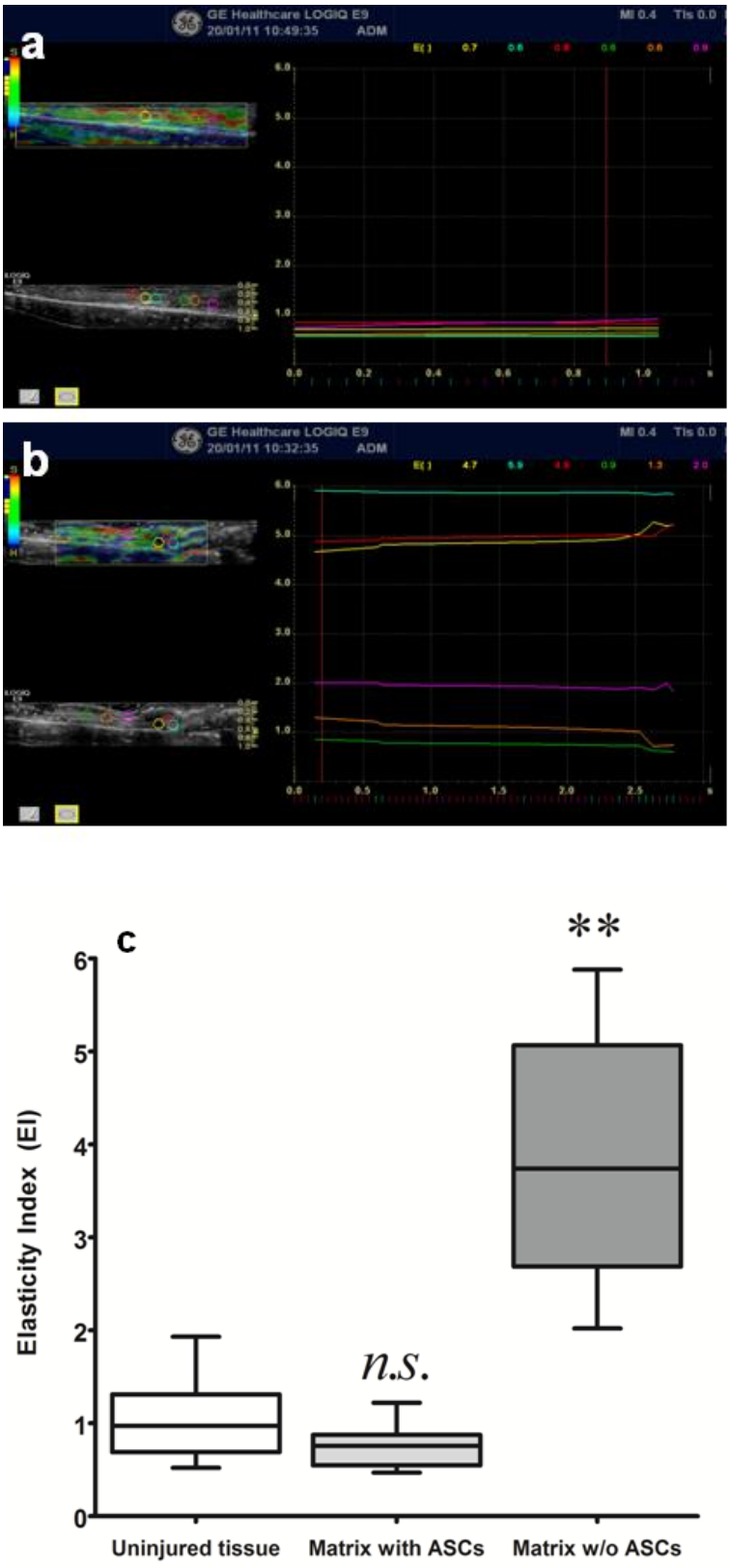

Figure 11: Example of sonoelastography for injured tendon tissue treated with stem cell seeded matrix (a) and unseeded matrix (b). Statistical analysis (c) revealed that autologous ASC treatment significantly lowered (**p<0,001) elasticity index of Achilles tendons (0.73, SD±0.26) compared to tendons treated with unseeded matrix (4.02, SD±1.33) but did not differ (n.s., p>0.05) from uninjured tendons (1.05, SD±0.40).

Repeated measures ANOVA with a Greenhouse-Geisser correction for each tendon group demonstrated no difference in EI measurements between all ten time points (p>0.05) (Figure 12) indicating a reproducible procedure with valid data inquiry.

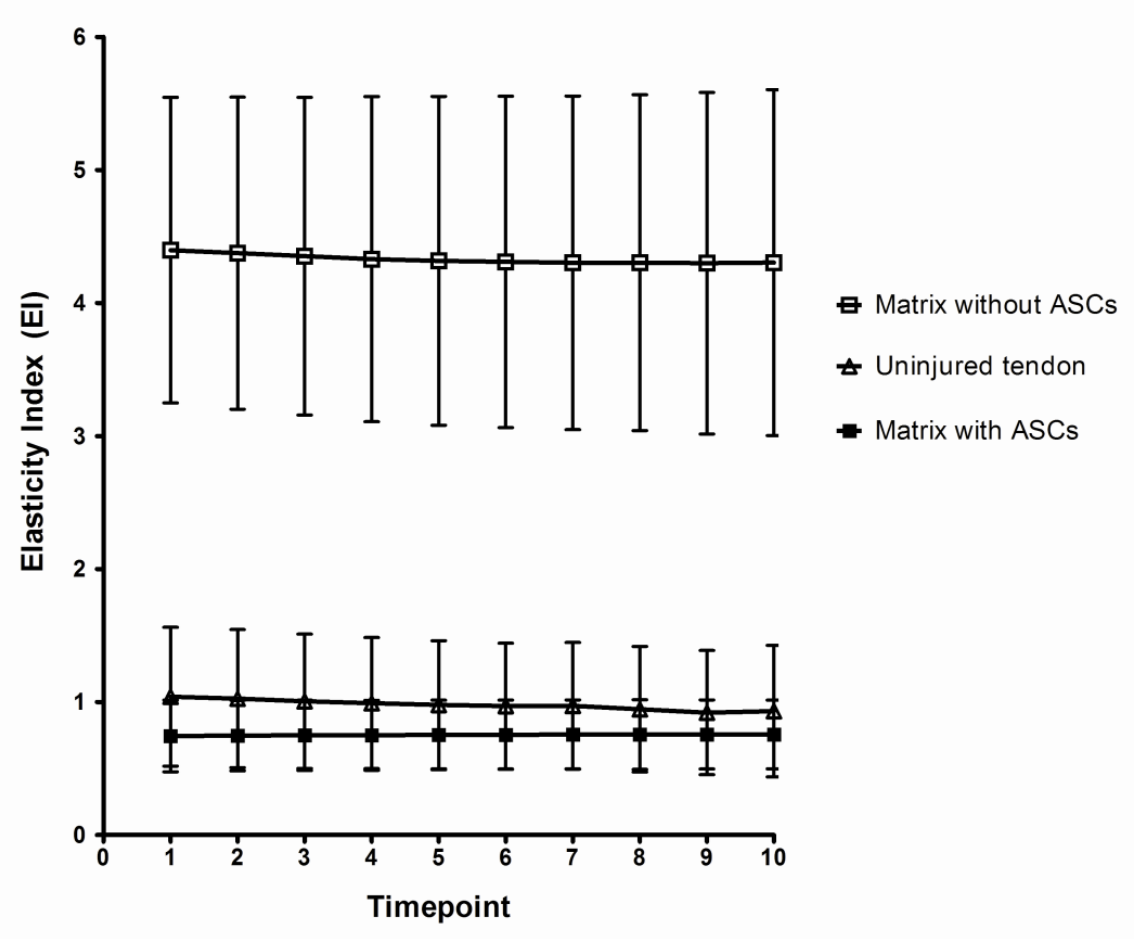

Figure 12: A repeated measures ANOVA for each tendon group determined that EI did not differ statistically significantly (p>0.05) between all ten time points (1-10) in each group. This demonstrates that tendon compression during elastographic measurement for each group gives reliable results independent of the time. Standard deviation of tendons treated with unseeded matrix (SD±1.33) were significantly higher (p<0.01) when compared to uninjured (SD±0.40) or ASC seeded matrix treated tendon tissue (SD±0.26).

Furthermore, the standard deviation of the elasticity index between uninjured tendons (SD±0.40) and stem cell treated tendons (SD±0.26) did not show a significant difference (p>0.05). Interestingly, standard deviation of tendons treated with unseeded matrix (SD±1.33) was significantly higher (p<0.01) when compared to uninjured or ASC seeded matrix treated tendon tissue.

7.4 Fluorescence microscopy

Fluorescence microscopy was performed for each tendon treated with DAPI labeled ASCs. All tissue sections were positive for labeled ASCs whereas no cells were apparent in adjacent tissue. Even after 8 weeks DAPI labeled cells were detected and showed successful engraftment after local application (Figure 13). In preliminary examination apoptosis and cytotoxicity was recognized as acceptable for a DAPI-concentration of 50µg/ml.

In the surrounding of ASCs Texas Red labeled collagen I could be detected (Figure 14).

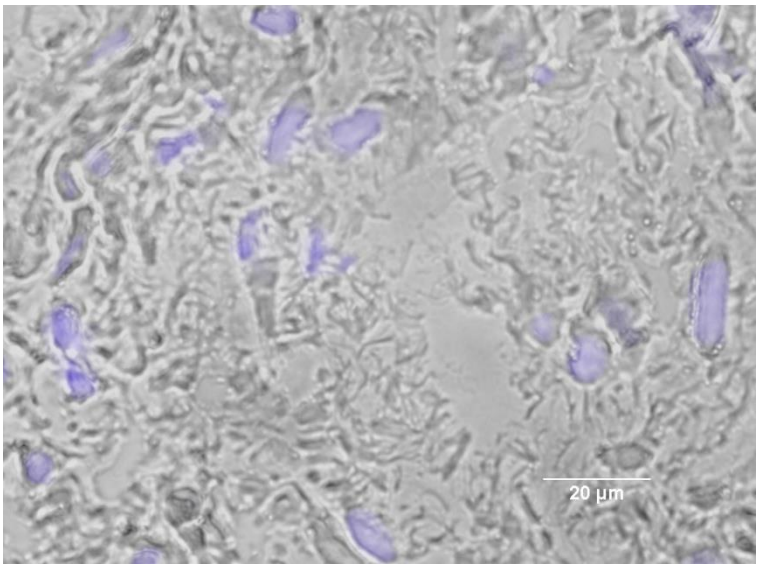

Figure 13: Overlay of phase-contrast and fluorescence microscopy of tendon tissue section 8 weeks after implantation. ASCs are labeled with DAPI and can be found throughout the tissue section.

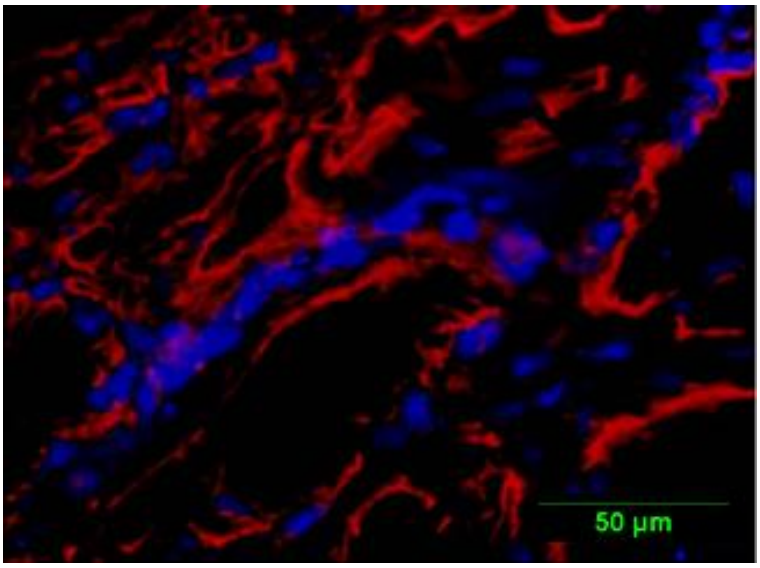

Figure 14: Fluorescence microscopy of tendon tissue section with DAPI labeled ASCs and Texas Red labeled collagen I antibody.

7.5 Histological examination

Histological examination of tendon tissue was performed 8 weeks after initial injury and demonstrated organized bands of collagen in both matrix treated groups and non-injured tendon tissue. No differences were observed regarding elongated cell morphology and parallel organization between groups treated with extracellular matrix seeded with stem cells (group 2) or without (group 3) (Figure 16). Moreover, no differences were apparent for Collagen I content between all groups (Figure 15).

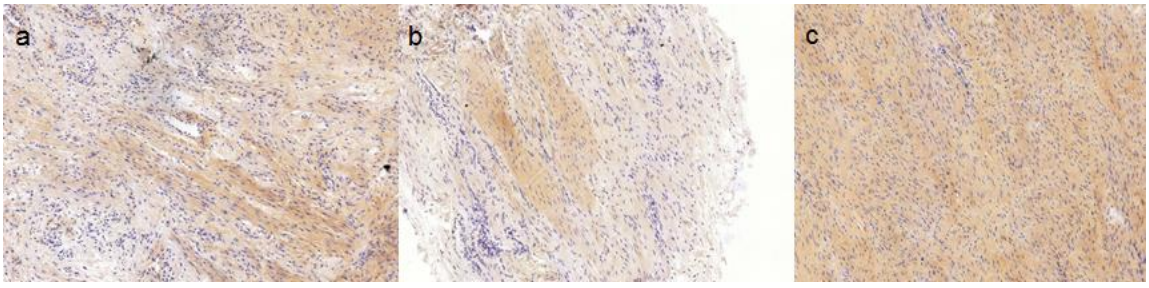

Figure 15: Immunohistochemistry of collagen I of (a) the control group (no injury) (b) matrix only (c) ASCs seeded matrix; (all 4x magnification)

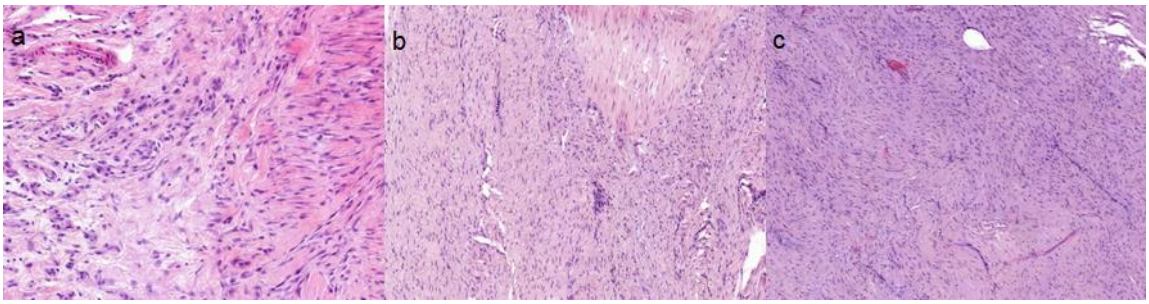

Figure 16: H&E staining of (a) the control group (10x magnification), (b) matrix only (5x magnification), (c) ASCs seeded matrix (4x magnification)

8. Discussion

The aim of the study was to investigate the effect of adipose-derived stem cells on tendon's elasticity and the capability of real time sonoelastographic examination to monitor tendon elasticity.

The major finding of the present study is that adipose derived stem cells embedded in extracellular collagen matrix have the capability to restore tendon's elasticity significantly after injury to the same level of uninjured tendon tissue. Furthermore, sonoelastography proved to be a valuable tool to monitor elasticity of Achilles tendon during tendon tissue regeneration.
In addition, sonoelastography is able to monitor the elastic properties of tendons in an examiner-independent and reproducible manner

Transdifferentiation of ASCs

The present study demonstrated that ASCs, yield from the same fat body as ASCs seeded on the collagen matrix, have the capability to differentiate into adipocytes and osteocytes in vitro.
These findings are consistent with previous studies showing that ASCs are able to retain the ability to differentiate into cell types of multiple different lineages like adipocyte, chondrocyte, myocyte, neuronal and osteoblast lineages[66].
Recently, Uysal et al.[47] demonstrated that ASCs differentiate into tenocytes in-vivo and pointed out that this finding might be a direct effect of applied ASCs to tendon healing. However, control and secretion of growth factors in the environmental tissue may also play a substantial role during primary tendon repair .This is supported by findings that ASCs are able to express tendon specific markers when treated with growth differentiation factor 5 [67].
The cellular constructs may have had different mechanical and physical properties as compared to the acellular constructs due to the applied cells which have caused differences in local microenvironment response.

The treatment of collagen composites with ASCs showed a significant higher elasticity than tissue repair without cells. However, this improvement did not correlate with cell morphology or parallel collagen organization in histological examination. Moreover, no differences were apparent for investigated Collagen content. This is in line with a previous study that investigated different stem cell densities on collagen matrices on a rabbit patellar tendon defect[49]. However, to date it is still under investigation whether cell differentiation of ASCs into tenocytes or growth factors expressed by ASCs is crucial for tendon tissue repair.

Sonoelastography and elasticity

The purpose of rehabilitation after tendon injury is to restore optimal tendon function, which requires re-establishment of tendon fibers and gliding mechanisms between tendon and its surrounding structures[68] while simultaneously preventing tendon rupture[69] as the most common complication during rehabilitation[70]. This is hindered by the limited self-repair capacity of tendon tissue, which is especially due to its cell-poor composition, its bradytrophic nature[10] and a low metabolic rate[11] which results in slow healing after injury. After tendon injury the formation of scar tissue occurs due to the proliferation phase in which synthesis of collagen III peaks[71] followed by the remodeling phase commencing with a higher proportion of synthesis of stronger[72] collagen I[73]. This is why the strength of the immature scar tissue from the proliferation phase increases during the remodeling phase. 11 weeks after tendon tissue injury a stepwise change of the fibrous tissue to scar-like tendon tissue occurs and last over the period of up to one year[74] during the maturation stage. Nevertheless ruptured tendon in its natural composition never regains the biomechanical properties prior to injury[75]. This scar-like tissue could be one reason of less elasticity in complete ruptured Achilles tendons as reported by Tan S. et. al.[64].

Not only stiffness and elasticity, respectively, or tendon's composite are parameters for tendon's mechanical function but also ultimate load, ultimate strain and tensile strength[16] . Alteration of these parameters, naturally evolve

during the process of aging, account for tendons susceptibility to tear when exposed to increasing stress[76].

To demonstrate efficient tendon regeneration regarding force transmission various studies have been investigated dynamic and static biomechanical properties[77], histological differences[78], ultimate load and stiffness[79], cross link density[80], collagen composition[81] and correlation of force with fibril diameter[82]. However, all described methods, evaluating indicators for tendon healing, are inapplicable for in vivo use and therefore are not suitable for clinical purposes. Moreover, preparation of histologic sections requires several days to weeks and includes animal-to-animal variations when making a static histologic assessment. In addition, recent studies suggest that histological changes might not be significant for time points after 6 weeks post-surgery[10,49]. These results stand in line with outcomes of this study as almost no differences could be determined between ASCs treated tendons, tendons without ASCs and uninjured tendons in the histological examination. This finding may indicate tendon's elasticity cannot be evaluated by histological examination and therefore other methods have to be used to provide a reliable source to monitor tendon regeneration or/and healing, especially for in vivo use.

Sonoelastography enables the evaluation of tendons' elasticity as a surrogate marker in vivo[64,83], as well as for other types of tissue. Thus, sonoelastography is already in clinical use for the evalutation of tumor morphology (e.g. breast, pancreas, prostate, thyroid), tissue stiffness, (e.g. liver fibrosis), and characterization of soft tissue lesion.[59–62,84–90] Studies support that although sonoelastography is not as established as ultrasound, it already offers a more precise localization of prostate carcinoma[90]. Moreover, studies reported an increased rate of detection for malignant thyroid nodules[88] and provided evidence that SE is superior to ultrasound in evaluating pancreatic masses[60]. Conventional ultrasound can be used as a diagnostic tool in the postoperative assessment of the ruptured Achilles tendon[91,92]. The round irregular area with mixed echogenicity as well as the increased size of the operated Achilles tendon rupture is well detected by ultrasound[93]. This correlates with the ultrasound examination of the present study as ultrasound could depict the former defect in all injured tendons.

In the present study each tendon group demonstrates equal EI measurements between all ten time points which suggests sonoelastography is not only suitable to monitor elasticity of Achilles tendon, which stand in line with other studies[64,83,94], but is able to do so in a reproducible, examiner-independent way, using the LOGIQ®E9 (General Electrics) software. Furthermore, this showed that the EI in the ROI is not affected by duration of pressure performed during the examination procedure. A major limitation of previous studies[64,95,96] is based on the interpretation and description of pattern and scores which required radiologist's experience. Furthermore, the evaluated elasticity in this present study was converted into a numerical value accurate to a tenth, using the LOGIQ®E9 (General Electrics) software, whereas other studies evaluated elasticity by a color grading system[64,83,96], differentiating only between 3 grades. The LOGIQ®E9 software not only provides reproducible but also more precise results compared to former studies. To achieve the most reproducible and precise outcome a region of interest was placed at the site of the defect. This is of great necessity, especially in the group without injury, since even the same tendon may show different stiffnesses at different anatomic locations[54]. Further studies have to examine Achilles tendon in vivo using the LOGIQ®E9 (General Electrics) software to confirm the present results collected in ex vivo examination.

Moreover, the EI of ASCs treated tendons was similar to the EI of uninjured tendons whereas EI for the collagen matrix alone treated tendons showed a much higher EI. This fact may indicate that real-time sonoelastography is suitable for the investigation of the healing process of the Achilles tendon since elasticity is an important function of tendon tissue[54]. In addition, this finding may further consider that a lower value of EI may reflect an improvement of the remodeling process with a decrease of scar-tissue. This is of interest since histological examination could not depict a clear difference regarding the size of scar tissue. Noteworthy, tendon elasticity has been reported to be correlated with late functional outcome in early stage of healing after injury[97].

Further investigation is needed to confirm whether sonoelastography is capable to monitor elasticity of tendons other than the Achilles tendon in the same reproducible and precise way.

Adipose derived stem cells and elasticity

Primary tendon repair aims to increase tensile strength and other biomechanical parameters for early mobilization and prevention of re-rupture. Therefore open and percutaneous suture techniques as well as operation techniques have been investigated [98,99]. Various authors have described modified suture techniques to increase the strength of primary repair[100,101]. In addition, stem cell application and matrix/scaffold implantation became a further approach to tendon repair by taking maximal advantage of natural healing processes.

In the present study adipose derived stem cells were yield from nuchal fat tissue and were seeded onto collagen matrixes. Histological no significant difference of elongated cell morphology and parallel organization of collagen between both matrix treated groups regarding stem cell application was detected. Moreover, no differences for the collagen I content were apparent. These results suggest that tendon's elasticity cannot be evaluated by histological examination due to almost similar properties after 8 weeks in all groups. The histological findings are in line with a previous report that showed no significant difference in cellular organization or histological appearance in a patellar tendon injury model at 6, 12 or 26 weeks after surgery[49]. However, bone marrow derived stem cells treated matrix were used and compared with natural healing for this study. Noteworthy, it has been demonstrated that biomechanical properties increased at a significantly faster rate for stem cell treated tendon tissue. Interestingly, Chong et. al.[37] could show that histomorphological differences, using bone marrow derived stem cells, were present only in time-points earlier than 6 weeks after injury. In contrast, Young et. al. reported more elongated cell morphology and parallel organization in stem cell-loaded matrix in Achilles tendon injury, however, controls were only treated with suture[40]. These findings suggest, that the applied matrix in a tendon repair model has a significant impact on histological appearance and has to be considered as an additional supportive effect regarding organization of extracellular compounds. On the other hand, Nixon et al. showed that solely the injection of stem cells improved linearity of collagen fibers and uniformity appearances in histological section when compared to PBS injection[102]. However, this study used collagenase I to

induce a tendinitis rather than an incision injury which might be the main reason for reported results.

Furthermore, the present study confirms that stem cell application successfully restores elastic properties of injured tendons (EI: 0.73, SD±0.26). Interestingly, elastic properties reached the same level as uninjured tendons (EI: 1.05, SD±0.40), whereas tendons treated with matrix only showed a significant higher EI (4.02, SD±1.33) when examined with LOGIQ®E9 (General Electrics) software. Tendon elasticity is one important marker regarding tendons biomechanical properties and is connected with tensile strength. Thus, the present results are supported by previous studies which showed an improvement of biomechanical properties due to mesenchymal stem cell application[35,40,49]. Uysal et al.[16] could show that ASCs, in particular, mixed with platelet-rich plasma improves tensile strength when placed between the defect. A recently published study could show that even an intra-tendinous injection of adipose derived stromal vascular fraction is able to increase biomechanical properties[51]. Moreover, a number of studies[40,103] have confirmed that scaffolds seeded with stem cells have better biomechanical properties than the implantation of constructs alone. These findings confirm the present results since tendons treated with matrix alone showed a much higher EI indicating a decrease of biomechanical property regarding elasticity.

Furthermore, the standard deviation of the elasticity index between the group of uninjured tendons (SD±0.40) and the group of stem cell treated tendons (SD±0.26) did not show a significant difference ($p>0.05$). Interestingly, standard deviation of tendons treated with unseeded matrix (SD±1.33) were significantly higher ($p<0.01$) when compared to uninjured or ASC seeded matrix treated tendon tissue. This might demonstrate a more precise predictive power for the outcome of elasticity after treating achilles tendon ruptures with ASC seeded matrix in comparison with unseeded matrix. Moreover, this suggests that applied ASCs minimize the risk of outliners, which in part is giving rise to a re-rupture rate after natural healing in human and other complications (e.g. longer rehabilitation time). This is of special interest, since histological investigation did not reveal any significant difference between both matrix groups.

The present fluorescence microscopic examination for the detection of DAPI-labeled ASCs revealed the presents of these cells in the area of defect at 8

weeks postoperatively whereas the labeled cells did not migrate into adjacent regions. This result is in line with a previous study using bone marrow derived stem cells[49]. The present results demonstrate that ASCs are able to integrate into an existing surrounding of united cell structure. ASCs can be applied easily to a tendon defect in a one-time procedure with improvement of elastic properties 8 weeks after surgery. The application of ASCs might be interesting for future consideration of Achilles tendon injury treatment since the early phase of tendon healing may predict the final outcome regarding elasticity[97].

Collagen type I synthesis is the key step in the determination of the tensile strength[16]. However, collagen type III initiates the healing process of tendons supplied by tenocytes and fibroblasts[104]. It was also shown that an increase of the collagen III content caused thinner collagen fibers and decreased the tensile strength at the same time[6]. Tang et al.[105] described an increase of collagen I gene expression at later periods of tendon healing in vivo than the expression of the collagen III gene. Most important it was revealed that ASCs mixed with platelet-rich plasma increases the amount of collagen I when compared to the control group treated with platelet-rich plasma alone[16]. In view of these facts further research will be necessary to prove the influence of ASCs on the content of collagen I and III regarding to elasticity. Therefore histology of different time points and, above all, a control group treated neither with ASCs nor with collagen matrix alone would be helpful as the present study only investigated the differences of two matrix treated groups at one time point. The fact that in this particular situation no correlation between elasticity and the content of collagen I could be demonstrated suggests that there will no correlation at any different time point. Nevertheless the development of collagen I in an untreated control group and its elasticity seems to be very interesting when compared with the other groups.

Moreover, histological examination at different time points of all groups would also be interesting for the questions whether DAPI-label ASCs stay at the same number or decrease. Concerning this matter Awad et al. showed that the intensity of fluorescence decreased with time after surgery, as did the number of stained bone marrow derived stem cells[49]. However, fluorescent cells were still apparent at the repair site at 26 weeks after surgery.

Further investigation will be necessary to show whether the density of applied ASCs to collagen matrix will affect elasticity or histological properties in any way. It was shown that different autologous mesenchymal stem cell concentrations (1, 4 and 8×106 cells/ml) in a type I collagen gel significantly improved tendon repair, but not in a dose-dependent manner[49]. Other authors showed that decreasing cell-to-collagen ratio by 20 times (from 0.8 to 0.04 M cells/mg collagen) improves cell viability in culture and improves biomechanics and histological appearance at 12 weeks postsurgery[106].

Ouyang and colleagues[107] found that poly-lactideco-glycolide (PLGA) was better compared to other synthetic biodegradable polymers in allowing MSCs to adhere and grow. Furthermore, they demonstrated that the structure and biomechanic properties of tendon repair in a rabbit Achilles tendon model was improved by the composite of bone marrow stromal cells and knitted PLGA scaffold[35]. Kryger et al.[108] performed in vivo and in vitro experiments to evaluate the role of bone marrow-derived MSCs, adipose-derived MSCs, tendon sheath fibroblasts and epitendon tenocytes in tendon engineering by seeding them into acellularized allogenic tendons as flexor tendon grafts using a rabbit model. Histologically, the seeded tendon grafts were indistinguishable between the different experimental groups. Because all 4 cell types showed similar growth patterns, it was suggested that successful in vivo implantation of the reseeded acellularized tendon grafts could be achieved using these cells.

Therefore, further studies on the investigation of elasticity should considered comparing different types of cells and scaffolds subdivided into experimental groups. In this way the influence of cells and scaffolds on tendon healing would be investigated in a more complete and differentiated way.

In line with this suggestions stands a published systematic review by Goh et al.[109], in which the applicability of implants seeded with cells in tendon repair and regeneration was assessed. However, the authors found that the ideal scaffold and cell source for tissue engineering remain uncertain.

9. Limitations

There are several limitations to the study. First of all, our study's population as well as every single population of all 3 groups (18 Achilles tendons in 9 rabbits, 6 tendons for every group) was relatively small. Therefore this should be addressed in further studies. Second, an in vivo examination of all tendons was not performed. Hence, no findings could be stated about a correlation between in vivo and ex vivo results. Third, no different seeding densities were applied to the collagen matrices. Thus, no information of how density would influence elasticity can be given. Fourth, the examination of the tendons 8 weeks after surgery might be a reason of the equal amount of collagen I seen in the immunohistology. Other time-points may show different amount of collagen I between the different groups.

It has been shown that the subcutaneous fat bodies from around the neck and between the scapulae in young rabbits are mostly brown fat tissue[110]. However it is also known that ASCs can be harvested in white and brown fat tissue with same multi-potent properties[111].However, liposuction or subcutaneous surgery in human is rather practiced at sites known for distribution of white adipose tissue. Thus, the present results are limited to the rabbit model and further research is required to compare ASCs from white and brown fat tissue regarding their role in tendon tissue repair.

10. Conclusion

Previous studies investigated treatment protocols to improve tendon healing, since the repair mechanisms in tendon tissue are limited.

The present study is the first to establish sonoelastography as a suitable tool to monitor tendons elasticity in a reproducible way and offers examiner-independent assessment of elasticity in Achilles tendon repair. Furthermore, sonoelastography allowed the examiner to proof for the first time that ASCs have the capability to restore elastic properties of injured Achilles tendon up to the same level of uninjured Achilles tendons.

In conjunctions with previous studies, our results showed the importance of stem cell treatment for tendon defects as an alternative approach to improve tissue healing. Application of ASCs to tendon tissue rupture site might be an opportunity to prevent re-ruptures and may lead to better condition for rehabilitation as well as a better outcome due to improved elasticity.

11. References

1. Metzl, J. A., Ahmad, C. S. & Levine, W. N. The ruptured Achilles tendon: operative and non-operative treatment options. *Curr Rev Musculoskelet Med* **1,** 161–164 (2008).
2. Wolfman, N. M. *et al.* Ectopic induction of tendon and ligament in rats by growth and differentiation factors 5, 6, and 7, members of the TGF-beta gene family. *J. Clin. Invest.* **100,** 321–330 (1997).
3. Wang, J. H.-C. Mechanobiology of tendon. *J Biomech* **39,** 1563–1582 (2006).
4. Hoffmann, A. & Gross, G. Tendon and ligament engineering in the adult organism: mesenchymal stem cells and gene-therapeutic approaches. *Int Orthop* **31,** 791–797 (2007).
5. Evans, J. H. & Barbenel, J. C. Structural and mechanical properties of tendon related to function. *Equine Vet. J.* **7,** 1–8 (1975).
6. Eriksen, H. A., Pajala, A., Leppilahti, J. & Risteli, J. Increased content of type III collagen at the rupture site of human Achilles tendon. *J. Orthop. Res.* **20,** 1352–1357 (2002).
7. Hampson, K., Forsyth, N. R., El Haj, A. & Maffulli, N. in *Topics in Tissue Engineering*
8. Chuen, F. S. *et al.* Immunohistochemical characterization of cells in adult human patellar tendons. *J. Histochem. Cytochem.* **52,** 1151–1157 (2004).
9. Bi, Y. *et al.* Identification of tendon stem/progenitor cells and the role of the extracellular matrix in their niche. *Nat. Med.* **13,** 1219–1227 (2007).
10. Stoll, C. *et al.* Healing parameters in a rabbit partial tendon defect following tenocyte/biomaterial implantation. *Biomaterials* **32,** 4806–4815 (2011).
11. Williams, J. G. Achilles tendon lesions in sport. *Sports Med* **3,** 114–135 (1986).
12. Aström, M. Laser Doppler flowmetry in the assessment of tendon blood flow. *Scand J Med Sci Sports* **10,** 365–367 (2000).
13. Gigante, A., Specchia, N., Rapali, S., Ventura, A. & de Palma, L. Fibrillogenesis in tendon healing: an experimental study. *Boll. Soc. Ital. Biol. Sper.* **72,** 203–210 (1996).
14. Ansorge, H. L., Adams, S., Birk, D. E. & Soslowsky, L. J. Mechanical, Compositional, and Structural Properties of the Post-natal Mouse Achilles Tendon. *Ann Biomed Eng* **39,** 1904–1913 (2011).
15. Voleti, P. B., Buckley, M. R. & Soslowsky, L. J. Tendon Healing: Repair and Regeneration. *Annual Review of Biomedical Engineering* **14,** 47–71 (2012).
16. Uysal, C. A., Tobita, M., Hyakusoku, H. & Mizuno, H. Adipose-derived stem cells enhance primary tendon repair: Biomechanical and immunohistochemical evaluation. *J Plast Reconstr Aesthet Surg* **65,** 1712–1719 (2012).
17. Majewski, M. *et al.* Improvement of tendon repair using muscle grafts transduced with TGF-β1 cDNA. *Eur Cell Mater* **23,** 94–101; discussion 101–102 (2012).
18. Molloy, T., Wang, Y. & Murrell, G. The roles of growth factors in tendon and ligament healing. *Sports Med* **33,** 381–394 (2003).
19. Kobayashi, M. *et al.* Expression of growth factors in the early phase of supraspinatus tendon healing in rabbits. *J Shoulder Elbow Surg* **15,** 371–377 (2006).
20. Wòjciak, B. & Crossan, J. F. The effects of T cells and their products on in vitro healing of epitenon cell microwounds. *Immunology* **83,** 93–98 (1994).
21. Frank, C., McDonald, D. & Shrive, N. Collagen fibril diameters in the rabbit medial collateral ligament scar: a longer term assessment. *Connect. Tissue Res.* **36,** 261–269 (1997).
22. Bergkvist, D., Åström, I., Josefsson, P.-O. & Dahlberg, L. E. Acute Achilles tendon rupture: a questionnaire follow-up of 487 patients. *J Bone Joint Surg Am* **94,** 1229–1233 (2012).
23. Soroceanu, A., Sidhwa, F., Aarabi, S., Kaufman, A. & Glazebrook, M. Surgical versus nonsurgical treatment of acute achilles tendon rupture: a meta-analysis of randomized trials. *J Bone Joint Surg Am* **94,** 2136–2143 (2012).
24. Zhang, F. *et al.* Effect of vascular endothelial growth factor on rat Achilles tendon healing. *Plast. Reconstr. Surg.* **112,** 1613–1619 (2003).

25. Lyras, D. N. *et al.* Effect of combined administration of transforming growth factor-b1 and insulin-like growth factor I on the mechanical properties of a patellar tendon defect model in rabbits. *Acta Orthop Belg* **76,** 380–386 (2010).
26. Gurtner, G. C., Callaghan, M. J. & Longaker, M. T. Progress and potential for regenerative medicine. *Annu. Rev. Med.* **58,** 299–312 (2007).
27. Weissman, I. L. Stem cells: units of development, units of regeneration, and units in evolution. *Cell* **100,** 157–168 (2000).
28. Uccelli, A., Moretta, L. & Pistoia, V. Immunoregulatory function of mesenchymal stem cells. *Eur. J. Immunol.* **36,** 2566–2573 (2006).
29. Gimble, J. M. Adipose tissue-derived therapeutics. *Expert Opin Biol Ther* **3,** 705–713 (2003).
30. Krampera, M., Pizzolo, G., Aprili, G. & Franchini, M. Mesenchymal stem cells for bone, cartilage, tendon and skeletal muscle repair. *Bone* **39,** 678–683 (2006).
31. Tapp, H., Hanley, E. N., Jr, Patt, J. C. & Gruber, H. E. Adipose-derived stem cells: characterization and current application in orthopaedic tissue repair. *Exp. Biol. Med. (Maywood)* **234,** 1–9 (2009).
32. da Silva Meirelles, L., Chagastelles, P. C. & Nardi, N. B. Mesenchymal stem cells reside in virtually all post-natal organs and tissues. *J. Cell. Sci.* **119,** 2204–2213 (2006).
33. Zuk, P. A. *et al.* Multilineage cells from human adipose tissue: implications for cell-based therapies. *Tissue Eng.* **7,** 211–228 (2001).
34. Salingcarnboriboon, R. *et al.* Establishment of tendon-derived cell lines exhibiting pluripotent mesenchymal stem cell-like property. *Exp. Cell Res.* **287,** 289–300 (2003).
35. Ouyang, H. W., Goh, J. C. H., Thambyah, A., Teoh, S. H. & Lee, E. H. Knitted poly-lactide-co-glycolide scaffold loaded with bone marrow stromal cells in repair and regeneration of rabbit Achilles tendon. *Tissue Eng.* **9,** 431–439 (2003).
36. Awad, H. A. *et al.* Autologous mesenchymal stem cell-mediated repair of tendon. *Tissue Eng.* **5,** 267–277 (1999).
37. Chong, A. K. S. *et al.* Bone marrow-derived mesenchymal stem cells influence early tendon-healing in a rabbit achilles tendon model. *J Bone Joint Surg Am* **89,** 74–81 (2007).
38. Ellera Gomes, J. L., da Silva, R. C., Silla, L. M. R., Abreu, M. R. & Pellanda, R. Conventional rotator cuff repair complemented by the aid of mononuclear autologous stem cells. *Knee Surg Sports Traumatol Arthrosc* **20,** 373–377 (2012).
39. Juncosa-Melvin, N. *et al.* The effect of autologous mesenchymal stem cells on the biomechanics and histology of gel-collagen sponge constructs used for rabbit patellar tendon repair. *Tissue Eng.* **12,** 369–379 (2006).
40. Young, R. G. *et al.* Use of mesenchymal stem cells in a collagen matrix for Achilles tendon repair. *J. Orthop. Res.* **16,** 406–413 (1998).
41. Nourissat, G. *et al.* Mesenchymal stem cell therapy regenerates the native bone-tendon junction after surgical repair in a degenerative rat model. *PLoS ONE* **5,** e12248 (2010).
42. Okamoto, N. *et al.* Treating Achilles tendon rupture in rats with bone-marrow-cell transplantation therapy. *J Bone Joint Surg Am* **92,** 2776–2784 (2010).
43. Ni, M. *et al.* Tendon-derived stem cells (TDSCs) promote tendon repair in a rat patellar tendon window defect model. *J. Orthop. Res.* **30,** 613–619 (2012).
44. Ju, Y.-J., Muneta, T., Yoshimura, H., Koga, H. & Sekiya, I. Synovial mesenchymal stem cells accelerate early remodeling of tendon-bone healing. *Cell Tissue Res.* **332,** 469–478 (2008).
45. Zhu, X., Shi, W., Tai, W. & Liu, F. The comparition of biological characteristics and multilineage differentiation of bone marrow and adipose derived Mesenchymal stem cells. *Cell Tissue Res.* **350,** 277–287 (2012).
46. De Ugarte, D. A. *et al.* Comparison of multi-lineage cells from human adipose tissue and bone marrow. *Cells Tissues Organs (Print)* **174,** 101–109 (2003).
47. Uysal, A. C. & Mizuno, H. Tendon regeneration and repair with adipose derived stem cells. *Curr Stem Cell Res Ther* **5,** 161–167 (2010).
48. Gimble, J. M. *et al.* In vitro Differentiation Potential of Mesenchymal Stem Cells. *Transfus Med Hemother* **35,** 228–238 (2008).

49. Awad, H. A. *et al.* Repair of patellar tendon injuries using a cell-collagen composite. *J. Orthop. Res.* **21,** 420–431 (2003).
50. Juncosa-Melvin, N. *et al.* Effects of mechanical stimulation on the biomechanics and histology of stem cell-collagen sponge constructs for rabbit patellar tendon repair. *Tissue Eng.* **12,** 2291–2300 (2006).
51. Behfar, M., Sarrafzadeh-Rezaei, F., Hobbenaghi, R., Delirezh, N. & Dalir-Naghadeh, B. Enhanced mechanical properties of rabbit flexor tendons in response to intratendinous injection of adipose derived stromal vascular fraction. *Curr Stem Cell Res Ther* **7,** 173–178 (2012).
52. Woo, S.-H., Tsai, T.-M., Kleinert, H. E., Chew, W. Y. C. & Voor, M. J. A biomechanical comparison of four extensor tendon repair techniques in zone IV. *Plast. Reconstr. Surg.* **115,** 1674–1681; discussion 1682–1683 (2005).
53. Smith, A. M. & Evans, D. M. Biomechanical assessment of a new type of flexor tendon repair. *J Hand Surg Br* **26,** 217–219 (2001).
54. Qi, J. *et al.* Interleukin-1beta increases elasticity of human bioartificial tendons. *Tissue Eng.* **12,** 2913–2925 (2006).
55. Ophir, J., Céspedes, I., Ponnekanti, H., Yazdi, Y. & Li, X. Elastography: a quantitative method for imaging the elasticity of biological tissues. *Ultrason Imaging* **13,** 111–134 (1991).
56. Lerner, R. M., Huang, S. R. & Parker, K. J. 'Sonoelasticity' images derived from ultrasound signals in mechanically vibrated tissues. *Ultrasound Med Biol* **16,** 231–239 (1990).
57. Klauser, A. S., Faschingbauer, R. & Jaschke, W. R. Is sonoelastography of value in assessing tendons? *Semin Musculoskelet Radiol* **14,** 323–333 (2010).
58. Lorenzen, J., Sinkus, R. & Adam, G. [Elastography: Quantitative imaging modality of the elastic tissue properties]. *Rofo* **175,** 623–630 (2003).
59. Gheonea, D. I. *et al.* Real-time sono-elastography in the diagnosis of diffuse liver diseases. *World J. Gastroenterol.* **16,** 1720–1726 (2010).
60. Giovannini, M. *et al.* Endoscopic ultrasound elastography for evaluation of lymph nodes and pancreatic masses: a multicenter study. *World J. Gastroenterol.* **15,** 1587–1593 (2009).
61. Barr, R. G. *et al.* Evaluation of breast lesions using sonographic elasticity imaging: a multicenter trial. *J Ultrasound Med* **31,** 281–287 (2012).
62. Xie, L. *et al.* Real-time elastography for diagnosis of liver fibrosis in chronic hepatitis B. *J Ultrasound Med* **31,** 1053–1060 (2012).
63. Pedersen, M., Fredberg, U. & Langberg, H. Sonoelastography as a diagnostic tool in the assessment of musculoskeletal alterations: a systematic review. *Ultraschall Med* **33,** 441–446 (2012).
64. Tan, S. *et al.* Real-time sonoelastography of the Achilles tendon: pattern description in healthy subjects and patients with surgically repaired complete ruptures. *Skeletal Radiol.* **41,** 1067–1072 (2012).
65. Chernak, L., Silder, A., Lee, K. & Thelen, D. The Use of Ultrasound Elastography to Assess Long-Term Tendon Remodeling and Mechanics Following Musculotendon Injury. in *Conference Proceedings of the Annual Meeting of the American Soc;2010, p793*
66. Gimble, J. & Guilak, F. Adipose-derived adult stem cells: isolation, characterization, and differentiation potential. *Cytotherapy* **5,** 362–369 (2003).
67. Park, A. *et al.* Adipose-derived mesenchymal stem cells treated with growth differentiation factor-5 express tendon-specific markers. *Tissue Eng Part A* **16,** 2941–2951 (2010).
68. James, R., Kesturu, G., Balian, G. & Chhabra, A. B. Tendon: biology, biomechanics, repair, growth factors, and evolving treatment options. *J Hand Surg Am* **33,** 102–112 (2008).
69. Lehfeldt, M., Ray, E. & Sherman, R. MOC-PS(SM) CME article: treatment of flexor tendon laceration. *Plast. Reconstr. Surg.* **121,** 1–12 (2008).
70. Majewski, M., Widmer, K. H. & Steinbrück, K. [Achilles tendon ruptures: 25 year's experience in sport-orthopedic treatment]. *Sportverletz Sportschaden* **16,** 167–173 (2002).
71. Oakes, B. Tissue healing and repair: tendons and ligaments. *In: Frontera WR, editor. Rehabilitation of sports injuries: scientific basis. Boston: Blackwell Science; 2003.* p 56–98

72. Doral, M. N. *et al.* Functional anatomy of the Achilles tendon. *Knee Surg Sports Traumatol Arthrosc* **18,** 638–643 (2010).
73. Abrahamsson, S. O. Matrix metabolism and healing in the flexor tendon. Experimental studies on rabbit tendon. *Scand J Plast Reconstr Surg Hand Surg Suppl* **23,** 1–51 (1991).
74. Hooley CJ, Cohen RE. A model for the creep behaviour of tendon. *Int J Biol Macromol 1* 123–132 (1979).
75. Leadbetter, W. B. Cell-matrix response in tendon injury. *Clin Sports Med* **11,** 533–578 (1992).
76. Vogel, H. G. Influence of maturation and age on mechanical and biochemical parameters of connective tissue of various organs in the rat. *Connect. Tissue Res.* **6,** 161–166 (1978).
77. Nagasawa, K., Noguchi, M., Ikoma, K. & Kubo, T. Static and dynamic biomechanical properties of the regenerating rabbit Achilles tendon. *Clin Biomech (Bristol, Avon)* **23,** 832–838 (2008).
78. Carpenter, J. E., Thomopoulos, S., Flanagan, C. L., DeBano, C. M. & Soslowsky, L. J. Rotator cuff defect healing: a biomechanical and histologic analysis in an animal model. *J Shoulder Elbow Surg* **7,** 599–605 (1998).
79. Dyment, N. A. *et al.* The relationships among spatiotemporal collagen gene expression, histology, and biomechanics following full-length injury in the murine patellar tendon. *J. Orthop. Res.* **30,** 28–36 (2012).
80. Frank, C., McDonald, D., Wilson, J., Eyre, D. & Shrive, N. Rabbit medial collateral ligament scar weakness is associated with decreased collagen pyridinoline crosslink density. *J. Orthop. Res.* **13,** 157–165 (1995).
81. Birk, D. E. & Mayne, R. Localization of collagen types I, III and V during tendon development. Changes in collagen types I and III are correlated with changes in fibril diameter. *Eur. J. Cell Biol.* **72,** 352–361 (1997).
82. Parry, D. A. The molecular and fibrillar structure of collagen and its relationship to the mechanical properties of connective tissue. *Biophys. Chem.* **29,** 195–209 (1988).
83. De Zordo, T. *et al.* Real-time sonoelastography findings in healthy Achilles tendons. *AJR Am J Roentgenol* **193,** W134–138 (2009).
84. Bai, M., Du, L., Gu, J., Li, F. & Jia, X. Virtual touch tissue quantification using acoustic radiation force impulse technology: initial clinical experience with solid breast masses. *J Ultrasound Med* **31,** 289–294 (2012).
85. Barr, R. G. & Zhang, Z. Effects of precompression on elasticity imaging of the breast: development of a clinically useful semiquantitative method of precompression assessment. *J Ultrasound Med* **31,** 895–902 (2012).
86. Jung, H. J., Hahn, S. Y., Choi, H.-Y., Park, S. H. & Park, H. K. Breast sonographic elastography using an advanced breast tissue-specific imaging preset: initial clinical results. *J Ultrasound Med* **31,** 273–280 (2012).
87. Kwon, D. R. & Park, G. Y. Diagnostic value of real-time sonoelastography in congenital muscular torticollis. *J Ultrasound Med* **31,** 721–727 (2012).
88. Mansor, M. *et al.* Role of ultrasound elastography in prediction of malignancy in thyroid nodules. *Endocr. Res.* **37,** 67–77 (2012).
89. Mansour, N., Stock, K. F., Chaker, A., Bas, M. & Knopf, A. Evaluation of parotid gland lesions with standard ultrasound, color duplex sonography, sonoelastography, and acoustic radiation force impulse imaging - a pilot study. *Ultraschall Med* **33,** 283–288 (2012).
90. Rausch, S., Alt, W., Arps, H., Alt, B. & Kälble, T. The utility of transrectal sonoelastography in preoperative prostate cancer assessment. *Med Ultrason* **14,** 182–186 (2012).
91. Aström, M. *et al.* Imaging in chronic achilles tendinopathy: a comparison of ultrasonography, magnetic resonance imaging and surgical findings in 27 histologically verified cases. *Skeletal Radiol.* **25,** 615–620 (1996).
92. Richards, P. J., Win, T. & Jones, P. W. The distribution of microvascular response in Achilles tendonopathy assessed by colour and power Doppler. *Skeletal Radiol.* **34,** 336–342 (2005).
93. Karjalainen, P. T., Ahovuo, J., Pihlajamäki, H. K., Soila, K. & Aronen, H. J. Postoperative MR imaging and ultrasonography of surgically repaired Achilles tendon ruptures. *Acta Radiol* **37,** 639–646 (1996).

94. De Zordo, T. *et al.* Real-time sonoelastography: findings in patients with symptomatic achilles tendons and comparison to healthy volunteers. *Ultraschall Med* **31,** 394–400 (2010).
95. Itoh, A. *et al.* Breast disease: clinical application of US elastography for diagnosis. *Radiology* **239,** 341–350 (2006).
96. Drakonaki, E. E., Allen, G. M. & Wilson, D. J. Real-time ultrasound elastography of the normal Achilles tendon: reproducibility and pattern description. *Clin Radiol* **64,** 1196–1202 (2009).
97. Schepull, T., Kvist, J., Andersson, C. & Aspenberg, P. Mechanical properties during healing of Achilles tendon ruptures to predict final outcome: a pilot Roentgen stereophotogrammetric analysis in 10 patients. *BMC Musculoskelet Disord* **8,** 116 (2007).
98. Chu, H. *et al.* [Effectiveness comparison between modified percutaneous suture and conventional open suture in repairing acute closed achilles tendon rupture]. *Zhongguo Xiu Fu Chong Jian Wai Ke Za Zhi* **26,** 708–711 (2012).
99. Hrnack, S. A., Crates, J. M. & Barber, F. A. Primary achilles tendon repair with mini-dorsolateral incision technique and accelerated rehabilitation. *Foot Ankle Int* **33,** 848–851 (2012).
100. Robertson, G. A. & al-Qattan, M. M. A biomechanical analysis of a new interlock suture technique for flexor tendon repair. *J Hand Surg Br* **17,** 92–93 (1992).
101. Pişkin, A. *et al.* [Tendon repair with the strengthened modified Kessler, modified Kessler, and Savage suture techniques: a biomechanical comparison]. *Acta Orthop Traumatol Turc* **41,** 238–243 (2007).
102. Nixon, A. J., Dahlgren, L. A., Haupt, J. L., Yeager, A. E. & Ward, D. L. Effect of adipose-derived nucleated cell fractions on tendon repair in horses with collagenase-induced tendinitis. *Am. J. Vet. Res.* **69,** 928–937 (2008).
103. Ouyang, H. W., Goh, J. C. H., Mo, X. M., Teoh, S. H. & Lee, E. H. The efficacy of bone marrow stromal cell-seeded knitted PLGA fiber scaffold for Achilles tendon repair. *Ann. N. Y. Acad. Sci.* **961,** 126–129 (2002).
104. Kajikawa, Y. *et al.* Platelet-rich plasma enhances the initial mobilization of circulation-derived cells for tendon healing. *J. Cell. Physiol.* **215,** 837–845 (2008).
105. Tang, J. B., Xu, Y., Ding, F. & Wang, X. T. Expression of genes for collagen production and NF-kappaB gene activation of in vivo healing flexor tendons. *J Hand Surg Am* **29,** 564–570 (2004).
106. Juncosa-Melvin, N. *et al.* Effects of cell-to-collagen ratio in mesenchymal stem cell-seeded implants on tendon repair biomechanics and histology. *Tissue Eng.* **11,** 448–457 (2005).
107. Ouyang, H., Goh, J., Mo, M., Teoh, S. & Lee, E. Characterization of anterior cruciate ligament cells and bone marrow stromal cells on various biodegradable polymeric films. *Mat Sci Eng C-BIO.* 63–69 (2002).
108. Kryger, G. S. *et al.* A comparison of tenocytes and mesenchymal stem cells for use in flexor tendon tissue engineering. *J Hand Surg Am* **32,** 597–605 (2007).
109. Goh, J. C.-H., Ouyang, H.-W., Teoh, S.-H., Chan, C. K. C. & Lee, E.-H. Tissue-engineering approach to the repair and regeneration of tendons and ligaments. *Tissue Eng.* **9 Suppl 1,** S31–44 (2003).
110. Hull, D. Structure and function of brown fat tissue. (1966).
111. Huang, S.-J. *et al.* Adipose-Derived Stem Cells: Isolation, Characterization and Differentiation Potential. *Cell Transplant* (2012). doi:10.3727/096368912X655127

12.Declaration

Ich erkläre, dass die der Medizinischen Fakultät der Universität Regensburg zur Promotion eingereichte Dissertation mit dem Titel

Application of adipose tissue-derived stem cells for restoration of achilles tendon elasticity after injury

selbstständig, ohne fremde Hilfe und ohne Benutzung anderer als der angegebenen Quellen und Hilfsmittel von mir angefertigt wurde. Alle Ausführungen, die wörtlich oder sinngemäß übernommen wurden, sind als solche gekennzeichnet.

Bei der Abfassung der Dissertation sind Rechte Dritter nicht verletzt worden. Diese Arbeit ist oder war nicht Gegenstand eines anderen Prüfungs- oder Promotionsverfahrens. Ich habe noch keinen Doktorgrad erlangt oder zu erlangen versucht. Ich übertrage der Medizinischen Fakultät das Recht, weitere Kopien meiner Dissertation herzustellen und zu vertreiben.

Regensburg, den 18.10.2016

13. Acknowledgements

First of all my biggest thanks goes to PD Dr. Sebastian Gehmert for his constantly patient and useful help and support during all the time. He thought me all necessary processes for working in the laboratory, built up all the connections to people helping me during my work and encouraged me throughout. Furthermore I acknowledge his critical reviews on my thesis.
Most of all, I want to show my respect for all the work he did simultaneously while always lending me an ear for my issues.

In addition, I would like to thank Dr. Ernst-Michael Jung, Department of Radiology, University Medical Center Regensburg, Regensburg, Germany. He helped me to examine the tendons with sonoelastography as well as analyzing all the data received during examination.

I also want to acknowledge Rudolf Jung for helping me making the slides for histological examination which he did alongside his daily work.

Thanks to Dr. Katharina Zeitler, Department of Pathology, University Medical Center Regensburg, Regensburg, Germany, for the results of the histological investigations.

My cordial thanks go to Prof. Dr. Lukas Prantl and Prof. Dr. Michael Nerlich, for the opportunity to work in his laboratory at the University Medical Center Regensburg, Germany.

I also want to acknowledge Carina Wenzl for her help and backup during the time in laboratory.

I would like to express my deepest gratitude and love to my parents and my brother. Their encouragement and support made all this possible.

14. Curriculum Vitae

Name:	Kügler
First name:	Tobias
Date of Birth:	December 24th, 1986
Place of Birth:	Gräfelfing
Citizenship:	German
Marital status:	unmarried

SCHOOL EDUCATION

09/1993-06/2006	Grundschule Gymnasium, Gröbenzell
2006	Abitur

ACADEMIC EDUCATION

10/2006-11/2012	Human Medicin, University of Regensburg

Clinical Rotation

04/2012-07/2012	Plastic Surgery Caritas Krankenhaus St. Josef, Regensburg, Germany University of Regensburg, Germany
12/2011-04/2012	Surgery Gesundheitszentrum Fricktal, Spital Rheinfelden, Switzerland University of Basel, Germany
08/2011-12/2011	Internal Medicine Addington Hospital, Durban, Southafrica University of KwaZulu-Natal, Southafrica

RESEARCH EXPERIENCE

6/2009-6/2011 Research Assistent
University of Regensburg, Deparment of Plastic Surgeery
Prof. Lukas Prantl
“Application of mesenchymal stem cells for restoration of achilles tendon elasticity after injury”

PROFESSIONAL EXPERIENCE

8/2013- assistant doctor at the Klinikum Augsburg, Department of Allgemein, Viszeral- und Transplantationschirurgie

PUBLICATIONS

Gehmert S., Jung E.M., Kügler T., Klein S., Gehmert S., Zeitler K., Loibl M., Prantl L. :Sonoelastography can be used to monitor the restoration of achilles tendon elasticity after injury Ultraschall Med. 2012 Dec; 33(6): 581-6

15. Addendum

15.1 Figures

treated with unseeded matrix (4.02, SD±1.33) but did not differ (n.s., p>0.05) from uninjured tendons (1.05, SD±0.40).

Figure 12 A repeated measures ANOVA for each tendon group determined that EI did not differ statistically significantly (p>0.05) between all ten time points (1-10) in each group. This demonstrates that tendon compression during elastographic measurement for each group gives reliable results independent of the time. Standard deviation of tendons treated with unseeded matrix (SD±1.33) were significantly higher (p<0.01) when compared to uninjured (SD±0.40) or ASC seeded matrix treated tendon tissue (SD±0.26).

Figure 13 Overlay of phase-contrast and fluorescence microscopy of tendon tissue section 8 weeks after implantation. ASCs are labeled with DAPI and can be found throughout the tissue section

Figure 14 Fluorescence microscopy of tendon tissue section with DAPI labeled ASCs and Texas Red labeled collagen I antibody

Figure 15 Immunhistochemistry of collagen I of (a) the control group (no injury) (b) matrix only (c) ASCs seeded matrix; (all 4x magnification)

Figure 16 H&E staining of (a) the control group (10x magnification), (b) matrix only (5x magnification), (c) ASCs seeded matrix (4x magnification)

15.2 Tables

Table 1 Compilation of cell therapies for tendon healing

Table 2 Preparation of 500 ml growth medium

Table 3 Preparation of 100 ml DAPI working solution

Table 18 Preparation of 100 ml antibody dilution buffer